

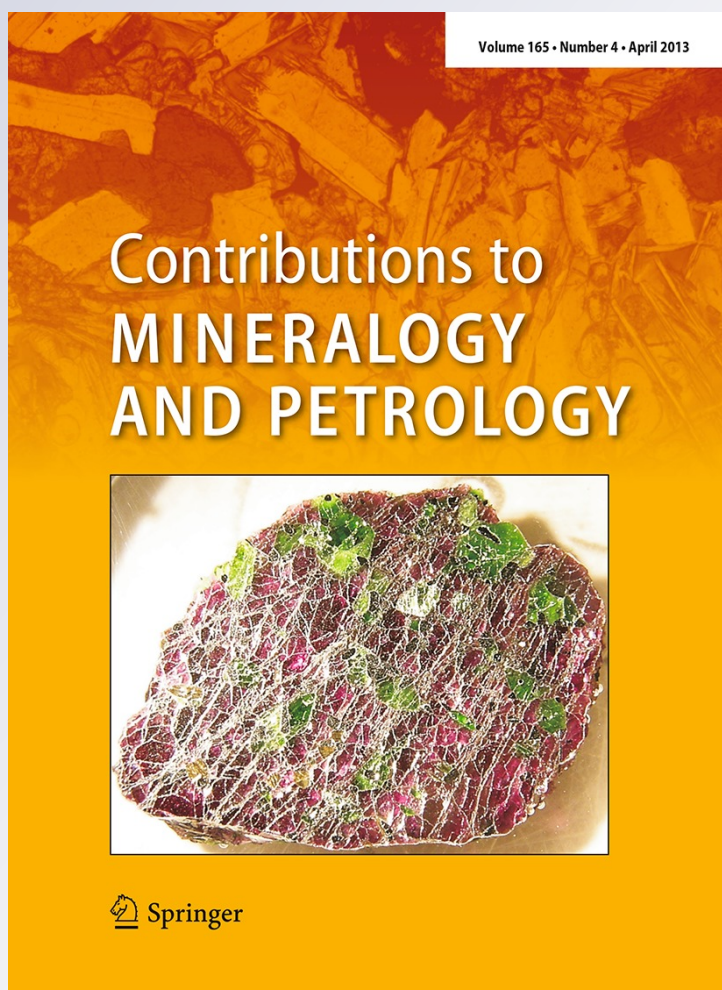
*Origin of the Tongbai-Dabie-Sulu
Neoproterozoic low- δ ^{18}O igneous province,
east-central China*

**Bin Fu, Noriko T. Kita, Simon A. Wilde,
Xiaochun Liu, John Cliff & Alan Greig**

**Contributions to Mineralogy and
Petrology**

ISSN 0010-7999
Volume 165
Number 4

Contrib Mineral Petrol (2013)
165:641-662
DOI 10.1007/s00410-012-0828-3



Your article is protected by copyright and all rights are held exclusively by Springer-Verlag Berlin Heidelberg. This e-offprint is for personal use only and shall not be self-archived in electronic repositories. If you wish to self-archive your work, please use the accepted author's version for posting to your own website or your institution's repository. You may further deposit the accepted author's version on a funder's repository at a funder's request, provided it is not made publicly available until 12 months after publication.

Origin of the Tongbai-Dabie-Sulu Neoproterozoic low- $\delta^{18}\text{O}$ igneous province, east-central China

Bin Fu · Noriko T. Kita · Simon A. Wilde ·
Xiaochun Liu · John Cliff · Alan Greig

Received: 23 July 2012 / Accepted: 30 October 2012 / Published online: 17 November 2012
© Springer-Verlag Berlin Heidelberg 2012

Abstract Zircons from 71 diverse rocks from the Qinling-Tongbai-Dabie-Sulu orogenic belt in east-central China and, for comparison, eight from adjoining areas in the South China and North China blocks, have been analyzed for in situ $^{18}\text{O}/^{16}\text{O}$ ratio and/or U–Pb age to further constrain the spatial distribution and genesis of Neoproterozoic low- $\delta^{18}\text{O}$ magmas, that is, $\delta^{18}\text{O}(\text{zircon}) \leq 4 \text{‰}$ VSMOW. In many metaigneous rock samples from Tongbai-Dabie-Sulu, including high-pressure and ultrahigh-pressure eclogites and associated granitic orthogneisses, average $\delta^{18}\text{O}$ values for Neoproterozoic “igneous” zircon cores (i.e., 800–600 Ma) vary from -0.9 to 6.9‰ , and from

-9.9 to 6.8‰ for Triassic metamorphic rims (i.e., 245–200 Ma). The former extend to values lower than zircons in primitive magmas from the Earth’s mantle (ca. 5–6 ‰). The average $\Delta^{18}\text{O}$ (metamorphic zircon – “igneous” zircon) values vary from -11.6 to 0.9‰ . The large volume of Neoproterozoic low- $\delta^{18}\text{O}$ igneous protoliths at Tongbai-Dabie-Sulu is matched only by the felsic volcanic rocks of the Snake River Plain hotspot track, which terminates at the Yellowstone Plateau. Hence, the low- $\delta^{18}\text{O}$ values at Tongbai-Dabie-Sulu are proposed to result from shallow subcaldera processes by comparison with Yellowstone, where repeated caldera-forming magmatism and hydrothermal alteration created similar low- $\delta^{18}\text{O}$ magmas. However, the possibility of involvement of meltwaters from local continental glaciations, rather than global Neoproterozoic glaciations, cannot be precluded. Our data indicate that Neoproterozoic low- $\delta^{18}\text{O}$ magmas that are either subduction- or rift-related are present locally along the western margin of the South China Block (e.g., Baoxing Complex). It appears that Neoproterozoic ^{18}O -depletion events in the South China Block as the result of hydrothermal alteration and magmatism affected a much larger area than was previously recognized.

Communicated by J. Hoefs.

Electronic supplementary material The online version of this article (doi:10.1007/s00410-012-0828-3) contains supplementary material, which is available to authorized users.

B. Fu (✉) · A. Greig
School of Earth Sciences, The University of Melbourne,
Parkville, VIC 3010, Australia
e-mail: binfu@unimelb.edu.au; mbinfu@bigpond.com

N. T. Kita
WiscSIMS, Department of Geoscience, University of Wisconsin,
Madison, WI 53706, USA

S. A. Wilde
Department of Applied Geology, Curtin University,
Perth, WA 6102, Australia

X. Liu
Institute of Geomechanics, Chinese Academy of Geological
Sciences, Beijing 100081, People’s Republic of China

J. Cliff
Centre for Microscopy, Characterisation and Analysis,
The University of Western Australia,
Crawley, WA 6009, Australia

Keywords Zircon · Oxygen isotopes · Ultrahigh-pressure metamorphism · Qinling-Tongbai-Dabie-Sulu orogenic belt · South China Block

Introduction

Zircon may preserve pristine igneous structures and compositions even in highly metamorphosed or hydrothermally altered rocks including oscillatory zoning as revealed by scanning electron microscopy—cathodoluminescence

(SEM–CL) imaging, magmatic ages, and chemical and/or isotopic compositions (e.g., Ti, REE—rare earth elements, Hf, Th, U, O). Thus, zircons provide unique information (e.g., age, fluid–rock interaction, temperature, and source) about the protolith or host rocks and their tectonic environment. For instance, the measured $\delta^{18}\text{O}$ values of igneous zircons commonly represent the oxygen isotope composition during crystallization of the magma (e.g., Lancaster et al. 2009; Fu et al. 2012). Post-magmatic exchange is retarded due to the slow diffusion of oxygen isotopes at crustal temperatures, and recrystallization as a result of metamorphism can be evaluated by U–Pb geochronology (e.g., Valley et al. 1994; Watson and Cherniak 1997; Valley 2003; Zheng et al. 2004; Page et al. 2007; Bowman et al. 2011). Furthermore, oxygen isotope zoning within single igneous zircons (e.g., core–rim structure) provides critical evidence to decipher complex overprinting events of magmatism and hydrothermal alteration (e.g., Bindeman et al. 2008a; Chen et al. 2011). A rapidly growing number of in situ oxygen isotope studies of zircons with ages from 4.4 Ga to <1 Ma in diverse rock types have been carried out by ion microprobe (secondary ion mass spectrometry, SIMS) to determine the evolution of the early Earth and later magmatism and metamorphism (e.g., Cavosie et al. 2005; Kemp et al. 2007; Trail et al. 2007; Harrison et al. 2008; Ickert et al. 2008; Chen et al. 2011; Dai et al. 2011; Grimes et al. 2011; Jeon et al. 2012).

Zircons in granitic orthogneisses associated with high- and ultrahigh-pressure (HP/UHP) eclogites from the Dabie–Sulu orogenic belt, eastern China, have a wide range in average $\delta^{18}\text{O}$ values from -9.0‰ to 6.2‰ VSMOW (e.g., Rumble et al. 2002; Zheng et al. 2004; Tang et al. 2008a, 2008b). Low $\delta^{18}\text{O}(\text{Zrn})$ in these rocks has been attributed to high-temperature exchange between Neoproterozoic igneous protoliths and isotopically light glacier meltwater during the Neoproterozoic glacial events (i.e., including the “snowball Earth”) (e.g., Rumble et al. 2002; Zheng et al. 2004, 2008). SIMS analyses of “igneous” zircon cores and so-called metamorphosed zircons in the eclogites and granitic orthogneisses indicate that $\delta^{18}\text{O}(\text{Zrn})$ varies from 0.1 to 10.1 ‰ (e.g., Chen et al. 2003, 2011). As discussed in detail by Wu et al. (2007), high-temperature hydrothermal alteration of the middle Neoproterozoic igneous rocks at Dabie resulted in low and negative $\delta^{18}\text{O}$ values for rock-forming minerals, and some of the altered rocks were locally melted to generate low- $\delta^{18}\text{O}$ magmas. Furthermore, the ^{18}O -depletion events took place at 780–740 Ma, and so they clearly predate the “snowball Earth” events (i.e., Sturtian and Marinoan) between 720 and 635 Ma (Zheng et al. 2007a, 2008 and references therein). Alternative explanations have also been discussed by Wang et al. (2011a) and Bindeman (2011). Thus, it appears that the occurrence of low- $\delta^{18}\text{O}$ magmas in the

South China Block during the Neoproterozoic may be unrelated to global glaciation events.

Numerous U–Pb zircon ages obtained by ID–TIMS (isotope dilution–thermal ionization mass spectrometry), SIMS, and LA–ICP–MS (laser ablation–inductively coupled plasma mass spectrometry) for rocks from the Tongbai–Dabie–Sulu orogenic belt have been published, and many of the U–Pb zircon age data were summarized in Zheng et al. (2003, 2008, 2009). In this contribution, we employed CAMECA IMS-1280 ion microprobes, combined with SIMS/LA–ICP–MS U–Pb dating, in order to obtain precise and accurate in situ analyses of oxygen isotope ratios in igneous and/or metamorphic zircons in diverse rocks obtained throughout the Tongbai–Dabie–Sulu orogenic belt, east-central China; we also included samples from adjacent areas in the South China and North China blocks for comparative purposes. The goal of this study was to further constrain the spatial distribution and genesis of low- $\delta^{18}\text{O}$ magmas in the Tongbai–Dabie–Sulu orogenic belt and to determine its tectonic, magmatic, and hydrothermal history prior to the Triassic HP/UHP eclogite-facies metamorphism.

Geological setting and sample descriptions

The Triassic continental collision between the North China Block and the South China Block in east-central China has generated the most extensive HP/UHP metamorphic province in the world. These rocks are exposed in the southern and eastern parts of the Qinling–Tongbai–Dabie–Sulu orogenic belt in a superterrane extending >1,500 km from west to east (inset of Fig. 1a). The most notable terranes are, from west to east, Tongbai, Hong’an (West Dabie), Dabie, and Sulu, which were disrupted by three major NNE–SSW trending faults, the Dawu and the Shangcheng–Macheng faults (DF and SMF; Fig. 1b) and the Tancheng–Lujiang or Tan-Lu Fault (TLF; Fig. 1a, b). These terranes expose a coherent sequence of subducted continental crust and cover now exhumed at the surface. The Hong’an, Dabie, and Sulu terranes contain both HP and UHP units, which were intruded by massive post-orogenic Cretaceous granites and minor mafic–ultramafic complexes. The UHP units consist of abundant ortho- and paragneiss, schist, marble, jadeite/kyanite quartzite, and minor eclogite lenses and garnet-bearing ultramafic complexes. The HP units mainly consist of gneiss, amphibolite, and eclogite. Coesite inclusions have been reported in zircons obtained from eclogites, particularly from associated gneisses (e.g., Ye et al. 2000; Liu et al. 2002; Liu and Liou 2011).

The Sulu terrane is bounded to the northwest by the Jiaobei terrane of the North China Block along the Wulian–Yantai Fault (WYF) and to the southeast by the South

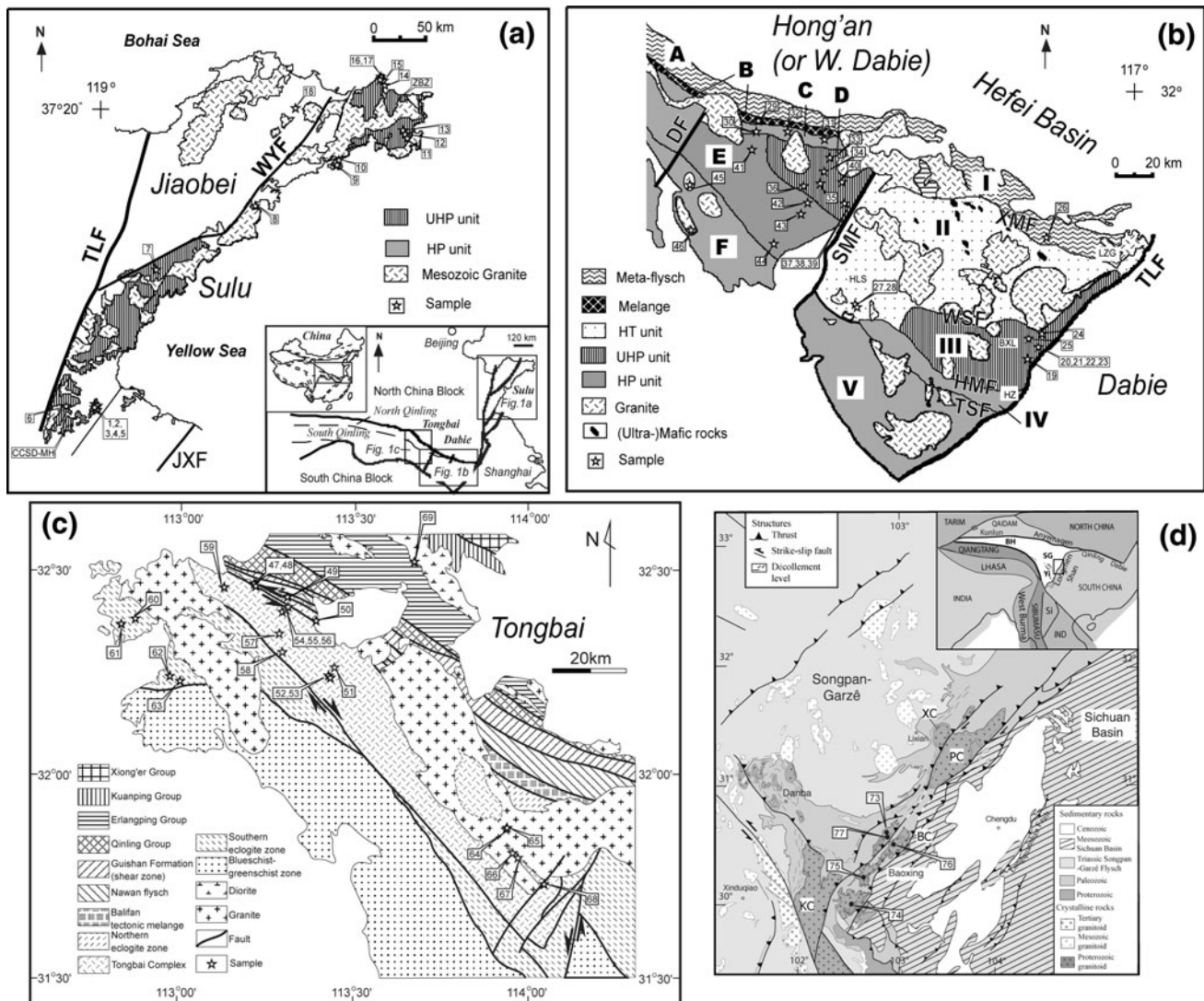


Fig. 1 Geological maps showing sample locations. The inset in (a) shows the location of the Qingling-Tongbai-Dabie-Sulu orogenic belt between the North China Block and the South China Block, east-central China, and the simplified geological maps show: **a** the Sulu terrane; **b** the Dabie terrane (including the Hong'an area or W. Dabie); and **c** the Tongbai terrane. Key localities include: ZBZ Zaubuzhen, Sulu, BXL Bixiling, HZ Huangzhen, HLS Huilanshan, LZG Luzhengan, from Dabie, and CCSD-MH—Chinese Continental Scientific Drilling—Main Hole, Sulu. See main text for abbreviations for faults and tectonic units. A schematic geological map of Longmenshan in

southwestern China is shown in **d** and its geographical position in the inset (figure courtesy of Y.T. Tian), modified after CIGMR (2004) and Roger et al. (2004). Abbreviations in (d): BC Baoxing Complex, PC Pengguan Complex, XC Xuelongbao Complex, KC Kangding Complex, and in the inset: SG Songpan-Garzê belt, BH Bayan Har terrane, Yi Yidun or Litang-Batang terrane, Si Simao terrane, IND Indochina. Note that three samples (#70–72) from South Qinling and two other miscellaneous samples (#78 and #79) from the South China and North China blocks (see Electronic supplementary materials S1) are not shown on the maps

China Block along the Jiashan-Xiangshui Fault (JXF) (Fig. 1a). Rocks of the HP unit in the Sulu terrane occur sporadically southeast of the UHP unit. The Precambrian basement in the Jiaobei terrane consists of Archean tonalite-trondhjemite-granodiorite (TTG) and supracrustal rocks including banded iron formation (BIF), and Paleoproterozoic amphibolite and granulite (Tang et al. 2007; Zhou et al. 2008 and references therein).

The Dabie terrane is divided into five lithotectonic units by E–W-trending faults, including the Xiaotian-Mozitan

Fault, the Wuhe-Shuihou Fault (shear zone), the Hualiangting-Mituo Fault, and the Taihu-Shanlong Fault (XMF, WSF, HMF, and TSF in Fig. 1b; Liu et al. 2007). From north to south, these units are the following (Zheng et al. 2008 and references therein): (I) the Beihuaiyang low-T/low-P greenschist-facies unit; (II) the North Dabie high-T/UHP granulite-facies unit; (III) the Central Dabie middle-T/UHP eclogite-facies unit; (IV) the South Dabie low-T/UHP eclogite-facies unit; and (V) the Susong low-T/high-P blueschist-facies unit (Fig. 1b).

In the Hong'an terrane, there are six lithotectonic units from north to south (Liu et al. 2004): (A) the Nanwan meta-flysch unit; (B) the Balifan mélange; (C) the Huwan HP unit; (D) the Xinxian UHP unit; (E) the Hong'an HP unit; and (F) the Mulanshan blueschist unit (Fig. 1b). The Nanwan flysch unit is composed of Devonian bedded quartz sandstone, pelite, and greywacke, and all the rocks are metamorphosed to greenschist or epidote–amphibolite facies. The Balifan tectonic mélange unit consists of augen mylonite, mylonitized quartzofeldspathic schist, and epidote amphibolite with many large metagabbro blocks. The Huwan HP unit comprises augen gneiss, mylonite, quartzofeldspathic schist, graphite schist, and marble with numerous eclogite blocks. The Xinxian UHP unit is a structural dome composed of granitic to granodioritic gneiss and minor supracrustal rock with abundant eclogite lenses or pods. The Hong'an HP unit consists of quartzofeldspathic schist, granitic orthogneiss, marble, quartzite, and graphite schist with layered garnet amphibolite, as well as eclogite and ultramafic blocks or lenses. The Mulanshan blueschist-greenschist unit is mainly composed of felsic and mafic volcanic rocks associated with metasedimentary phosphorite, graphite schist and quartzite in the lower part, and metapelite and marble in the upper part.

The Tongbai terrane represents the middle segment of the Qinling-Tongbai-Dabie-Sulu orogenic belt. It is separated from Qinling in the west by the Nanyang Basin, and from Hong'an in the east by the Dawu Fault. The terrane comprises six collision-related lithotectonic units, separated by large-scale shear zones (Liu et al. 2008, 2010a). From northeast to southwest, they are: (1) the Nanwan flysch, (2) the Balifan tectonic mélange, (3) the northern eclogite zone, (4) the Tongbai Complex, (5) the southern eclogite zone, and (6) the blueschist-greenschist zone (Fig. 1c). A coesite-bearing eclogite zone is, however, absent. Eclogites from the two eclogite zones commonly occur as lenses or blocks of a few to several hundreds of meters in size in quartzofeldspathic gneisses, mica schists, and marbles. The Tongbai Complex is dominated by coarse-grained gneissic granites. Most of these rocks were strongly deformed and commonly converted to augen gneisses and mylonites. The enclaves in the gneissic and weakly foliated granites comprise fine-grained dioritic-trondhjemitic gneisses and minor amphibolites, paragneisses, calc-silicates, and marbles. The dioritic-trondhjemitic gneisses are layered and commonly show granitic and pegmatitic veins. Amphibolites occur as interlayers or lenses within the dioritic-trondhjemitic gneisses.

The Baoxing Complex is located in the southern Longmenshan, while the Pengguan and Xuelongbao complexes lie to the north, between the Tibet Plateau and the Sichuan Basin in southwestern China (Fig. 1d). It consists mainly of highly deformed mafic to felsic (gabbroic,

dioritic, tonalitic, granodioritic, and monzogranitic) gneisses. The Neoproterozoic igneous rocks were emplaced into the Yanjing Group that is composed of an intermediate-acidic to alkaline volcanic complex, pelitic clastic rocks, and carbonates (BGMRS 1991). The cover sequences in this area include a thin, incomplete succession of Neoproterozoic to Middle Triassic shallow-marine and non-marine sedimentary rocks (Burchfiel et al. 1995). All the Precambrian basement rocks and the cover sequences were folded/deformed and metamorphosed to greenschist or amphibolite facies during the early Mesozoic. The massive tonalitic gneiss consists mainly of plagioclase, quartz, biotite, and minor amphibole and K-feldspar.

Zircons from 71 samples were chosen for analysis (Fig. 1): 17 samples from Sulu; 10 from Dabie; 18 from Hong'an; 23 from Tongbai; and 3 from South Qinling (e.g., Hannan Massif). The majority of the investigated samples are metaigneous rocks, including metagabbro, HP/UHP eclogite, garnet amphibolite, and granitic (or dioritic/trondhjemitic/quartzofeldspathic) orthogneiss from different lithotectonic units in the four terranes of the Tongbai-Dabie-Sulu orogenic belt. Metasedimentary rocks including paragneiss, schist, quartzite, and felsic granulite that may contain detrital zircons, as well as pre-orogenic intrusions, syn-orogenic (Triassic) pegmatitic dikes (Wallis et al. 2005), and post-orogenic Cretaceous intrusions (Liu et al. 2010a; Cui et al. 2012) were selected for comparison (Electronic supplementary materials or ESM S1). In addition, six samples from southern Longmenshan (e.g., Baoxing Complex) and Yichang (Huangling Granitoid) in the South China Block and two samples from the southern margin of the North China Block were also analyzed.

Analytical methods

For some samples, oxygen isotope analyses of garnet, amphibole, zoisite, and/or quartz were performed in bulk on 1–2 milligram-size samples using laser fluorination ($\lambda = 10.6 \mu\text{m}$, BrF_5) and gas-source mass spectrometry at the University of Wisconsin—Madison (Valley et al. 1995). The $^{18}\text{O}/^{16}\text{O}$ ratios are reported in δ notation relative to Vienna Standard Mean Ocean Water (VSMOW). All $\delta^{18}\text{O}$ values were corrected using the accepted values of the standards employed: 5.80 ‰ for UWG-2, Gore Mountain garnet standard (Valley et al. 1995), and 9.59 ‰ for NBS-28 quartz standard, and they are tabulated in Electronic ESM S2. All the data are reported here with uncertainty within 2 standard deviations (2 SD) or at the 95 % confidence levels (c.l.).

Zircon separates were obtained by standard crushing, magnetic, and heavy liquid techniques and were then handpicked under a binocular microscope. Unknown

zircon (and quartz) grains together with zircon standards (KIM-5, CZ3, Temora-2, and/or Plešovice) (and quartz standard, UWQ-1) were cast in epoxy, ground, and polished to expose the midsection of the grains. Nine 25-mm round zircon grain mounts were prepared, together with 11 other mounts previously prepared for in situ U–Pb zircon dating by ion microprobe (Liu et al. 2004, 2008, 2010a; Wallis et al. 2005; Cui et al. 2012; Hu et al. 2012); some of the mounts were face-mounted with KIM-5 or Plešovice in the center, and many of the previous geochronology pits were ground off.

Secondary electron and cathodoluminescence imaging of the zircons was conducted using a Hitachi S-3400N scanning electron microscope at the University of Wisconsin—Madison, or a Philips (FEI) XL30 ESEM (environmental SEM) at the University of Melbourne, both equipped with a Gatan CL detector. Representative CL images of the zircons of interest are shown in Fig. 2 and indicate that many zircons display core–rim structures: Zircon cores commonly exhibit oscillatory zoning in CL, whereas zircon rims tend to be weakly zoned or featureless.

Ion microprobe analyses of $^{18}\text{O}/^{16}\text{O}$ ratios in zircons were made using 10–15 μ spots on a CAMECA IMS-1280 ion microprobe with multi-collector Faraday Cups (FC) in

the WiscSIMS Laboratory at the University of Wisconsin—Madison (Kita et al. 2009). Ion microprobe analyses of $^{18}\text{O}/^{16}\text{O}$ ratios in zircons and quartz grains were also performed on a CAMECA IMS-1280 ion microprobe at the University of Western Australia; analytical procedures and data reduction were similar to those reported in Kita et al. (2009). All oxygen isotope results on samples and standards including KIM-5 ($\delta^{18}\text{O} = 5.09 \pm 0.12 \text{ ‰}$; Valley 2003), Plešovice ($8.19 \pm 0.08 \text{ ‰}$; J.W. Valley unpublished data), Temora-1 ($7.93 \pm 0.08 \text{ ‰}$; Valley 2003; Black et al. 2004), and Temora-2 ($8.20 \pm 0.02 \text{ ‰}$; Valley 2003; Black et al. 2004) as well as UWQ-1 (quartz, $12.33 \pm 0.14 \text{ ‰}$; Kelly et al. 2007) are listed in order of analysis in ESM S3. Optical microscope photographs of the oxygen isotope SIMS spots were taken and digitized, and/or post-analysis SEM imaging of many of the SIMS spots was performed to evaluate the reliability of in situ ion microprobe data.

After grinding off previous SIMS spots for $^{18}\text{O}/^{16}\text{O}$ ratio, the U, Th, and Pb compositions and U–Pb isotopic ratios for some of the zircons were obtained from newly polished, gold-coated zircon grain mounts using a SHRIMP II ion microprobe at the John de Laeter Centre of Mass Spectrometry, Curtin University, Perth. The operating conditions and analytical protocols using seven-cycle runs through the

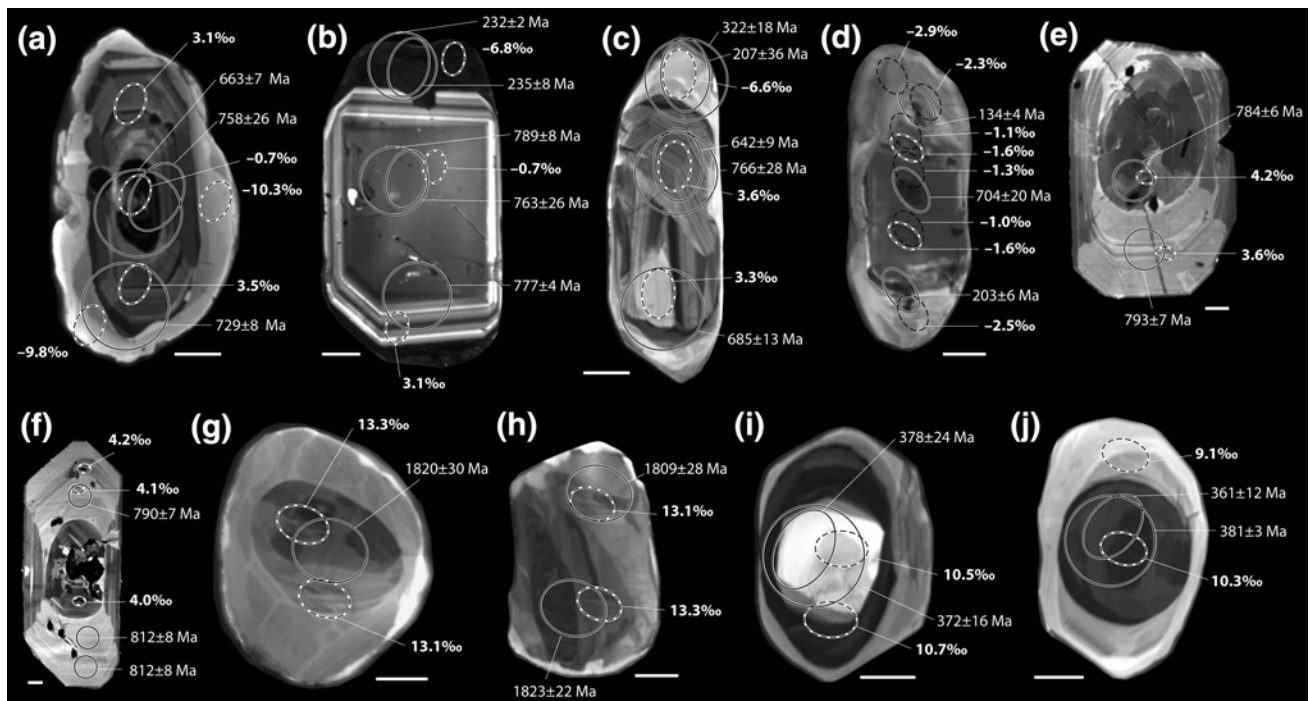


Fig. 2 Representative CL images showing zircons in rocks from the Tongbai-Dabie-Sulu orogenic belt: **a** grain no. 5, sample #2; **b** grain no. 3, sample #3; **c** grain no. 6, sample #20; **d** grain no. 15, sample #53; **e** grain no. 2, sample #73; **f** grain no. 3, sample #77; **g** and **h** grain nos. 1 and 6, sample #50; and **i** and **j** grain nos. 13 and 14, sample #30. Solid ellipses denote SIMS dating spots and dashed ones $^{18}\text{O}/^{16}\text{O}$ -analysis sites; circles represent LA-ICP-MS dating

sites. Note that the zircons **a–d** have contrasting $\delta^{18}\text{O}$ values between Neoproterozoic “igneous” zircon cores and Triassic metamorphic zircon rims, varying by up to 13.3 ‰, whereas the zircons **e–j** are relatively homogeneous in $\delta^{18}\text{O}$, and that six additional analyses of the zircon **d** for $^{18}\text{O}/^{16}\text{O}$ were performed after repolishing. Scale bars are 20 μm . The U–Pb ages and oxygen values are presented for each analytical site

mass stations are essentially the same as described by Williams (1998). The SHRIMP spots were ca. 25 μm in diameter. The Pb/U calibration was performed using the in-house CZ3 standard zircon ($^{206}\text{Pb}/^{238}\text{U}$ age = 564 Ma; Pidgeon et al. 1994), which was analyzed repeatedly throughout each session. All raw SIMS data files were reduced using the Squid program (Ludwig 2001a) and relative probabilities plotted using Isoplot/Ex (Ludwig 2001b). Apparent ages include uncertainty in the Pb/U calibration, and all errors are quoted at 2 SE (standard error) precision (ESM S4). Four zircon grains from sample (#44; Mount G72) were analyzed for U–Th–Pb isotopes using a SHRIMP II ion microprobe at the Institute of Geology, Chinese Academy of Geological Sciences, Beijing (cf. Liu et al. 2004).

Laser ablation U–Th–Pb isotope analyses of many of the studied zircons were carried out at the University of Melbourne, using a 193-nm excimer laser-based HELEX ablation system equipped with a Varian 810 quadrupole ICP–MS described in Woodhead et al. (2004, 2007) and Paton et al. (2010) and also using an Agilent 7700 ICP–MS. U–Th–Pb isotopic abundances were analyzed using a 32 μm spot size. All data manipulation was done off-line using the locally developed Iolite software package (Hellstrom et al. 2008) with the U–Th–Pb data reduction module of Paton et al. (2010). The results were calibrated with the 91500 zircon (Wiedenbeck et al. 1995) as the primary standard and are tabulated in ESM S5, and the weighted mean $^{206}\text{Pb}/^{238}\text{U}$ ages were obtained from two secondary standard zircons Temora-2 (415.9 ± 1.1 Ma, $n = 54$; 419.2 ± 1.4 Ma, $n = 68$) and Plešovice (338.8 ± 0.9 Ma, $n = 33$; 339.4 ± 0.7 Ma, $n = 90$) in two sessions and are well within $\pm 1.0\%$ of the accepted ages (416.8 and 337.1 Ma; Black et al. 2004; Sláma et al. 2008).

The initial common Pb isotopic composition of the analyzed zircons from different rocks was estimated using the two-stage terrestrial Pb evolution model of Stacey and Kramers (1975) at a given age; however, only radiogenic $^{207}\text{Pb}/^{206}\text{Pb}$ ages for zircons older than 1.2 Ga are presented.

Oxygen isotope compositions

Laser fluorination bulk analyses

Mineral separates analyzed by laser fluorination are from HP/UHP eclogites and jadeite quartzite at Dabie–Sulu (ESM S2). Garnet from the HP/UHP eclogites has a large range in $\delta^{18}\text{O}$ from -8.1 to 9.4% .

Coexisting minerals were analyzed in order to determine the extent of isotopic disequilibrium and fluid–“buffered” open system exchange (i.e., Valley 2001; Zheng et al.

2003). For an individual rock sample, compared to garnet, the coexisting omphacite, amphibole, and zoisite commonly have a slightly higher $\delta^{18}\text{O}$ value, as evident by positive $\Delta^{18}\text{O}(\text{Min–Grt})$ values, ranging between 0.17 and 0.86 ‰ (Fig. 3). Here, $\Delta^{18}\text{O}(\text{Min–Grt}) = \delta^{18}\text{O}(\text{Min}) - \delta^{18}\text{O}(\text{Grt})$, and Min stands for omphacite, zoisite, or amphibole and Grt for garnet. Oxygen isotope fractionation between omphacite (diopside₄₀–jadeite₆₀), zoisite, or amphibole (glaucophane) and garnet at $T = 700\text{ }^\circ\text{C}$ (or higher) using the calibrations of Zheng (1993a, b) is estimated to be ca. 1 ‰ or less. Within the accuracy of these estimates, the small oxygen isotope fractionations measured between these minerals suggest that the value for high-temperature isotopic equilibrium has been attained and preserved at peak-HP/UHP metamorphic conditions (e.g., Yui et al. 1995; Zheng et al. 1996, 1998a, 2003; Baker et al. 1997; Rumble and Yui 1998).

Ion microprobe spot analyses

Results of all SIMS spot analyses of unknown zircons are shown in Fig. 4, and individual $\delta^{18}\text{O}$ data for all the investigated samples are summarized in ESM S1. Nine analyses of seven quartz grains from one granitic orthogneiss sample (#6) that are not shown in Fig. 4 give a narrow range in $\delta^{18}\text{O}$ from -1.9 to -1.3% , averaging $-1.6 \pm 0.4\%$.

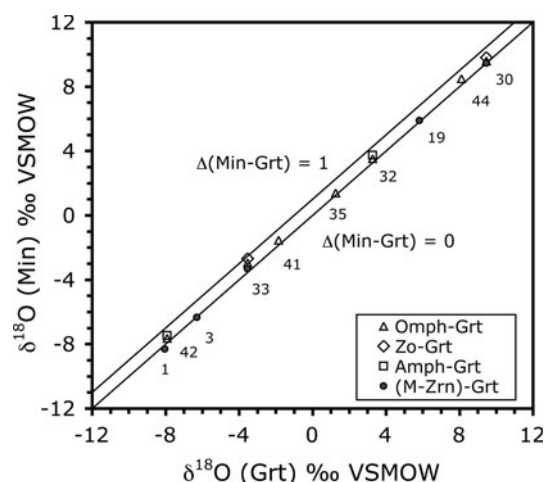
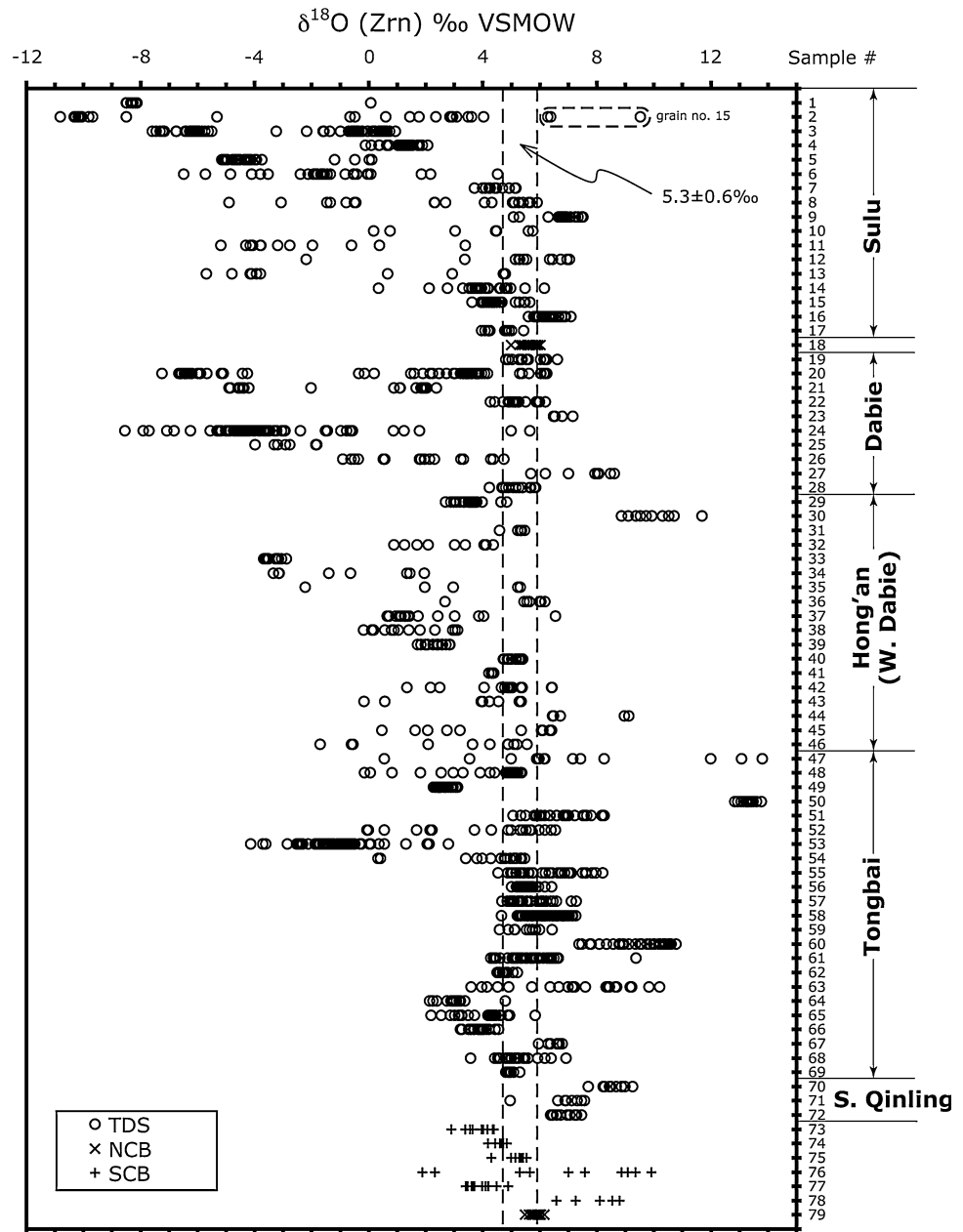


Fig. 3 Plot of $\delta^{18}\text{O}(\text{Min})$ versus $\delta^{18}\text{O}(\text{Grt})$ for some of the investigated samples from the Tongbai–Dabie–Sulu orogenic belt, analyzed by laser fluorination. Average $\delta^{18}\text{O}$ for metamorphic zircons ($n \geq 4$) from five rock samples analyzed by ion microprobe is also plotted; $2\text{ SD} \leq \pm 0.8\%$, comparable to the analytical precision, $\leq \pm 0.4\%$. Note that all data points fall between $\Delta^{18}\text{O}(\text{Min–Grt}) = 1$ and 0. Abbreviations: *Omph* omphacite, *Zo* zoisite, *Amph* amphibole, and *M-Zrn* metamorphic zircon. $\delta^{18}\text{O}(\text{Grt})$ for samples (#3 and #19) was taken from Zheng et al. (1998b) and Fu et al. (1999), respectively. See Electronic supplementary materials S1 for sample numbers

Fig. 4 Oxygen isotope ratios measured in situ by ion microprobe for zircons in rocks from the Qinling-Tongbai-Dabie-Sulu orogenic belt and adjacent areas. Vertical lines at 4.7 and 5.9 ‰ define the normal $\delta^{18}\text{O}$ range for zircon in high-temperature equilibrium with mantle compositions. Abbreviations: *Zrn* zircon, *TDS* Tongbai-Dabie-Sulu, *NCB* North China Block, *SCB* South China Block. The numbers (1–79) along the right vertical axis denote samples as listed in Electronic supplementary materials S1



The lowest $\delta^{18}\text{O}$ value for zircon is -10.8 ‰ from one UHP eclogite sample (#2), and the highest $\delta^{18}\text{O}$ value is 13.8 ‰ from one HP eclogite sample (#47) and one Paleoproterozoic pelitic schist sample (#50).

Zircons from some metagneous or igneous rock samples, especially from Hong'an and Tongbai (e.g., #33, #40, and #69), have a narrow range in $\delta^{18}\text{O}$, varying by only 0.2 to 0.8 ‰ (Fig. 4). This indicates $^{18}\text{O}/^{16}\text{O}$ -homogeneity in zircons at hand specimen scale. The intergrain variability can also be evaluated by a 2 SD value of average $\delta^{18}\text{O}(\text{Zircon})$ or $\delta^{18}\text{O}(\text{Zrn})$ for some individual rock samples (e.g., ± 0.1 to ± 0.5 ‰; ESM S1), comparable to the

analytical precision of ± 0.4 ‰. On the other hand, $\delta^{18}\text{O}$ in zircons from some other granitic orthogneiss/eclogite samples, notably from Dabie and Sulu (e.g., #2), can be highly variable by up to 20.4 ‰. The 2 SD value of the average $\delta^{18}\text{O}(\text{Zrn})$ for the metagneous rocks is as high as ± 7.0 ‰ (#47) and ± 9.1 ‰ (#20). It is noted that the 2 SD value of the average $\delta^{18}\text{O}(\text{Zrn})$ for most individual samples other than eclogites and orthogneisses is ± 2.2 ‰ or less. Many zircons from metagneous rocks have much higher $\delta^{18}\text{O}$ values in the core than in the rim (Figs. 2a–c). Since the distinction between “igneous” zircons and “metamorphic” zircons is not always straightforward, intragrain and

intergrain variability in $\delta^{18}\text{O}$ was based on CL images and U–Th–Pb results and is assessed in the “Discussion” section.

Average $\delta^{18}\text{O}(\text{Zrn})$ values for the investigated rocks at Qinling–Tongbai–Dabie–Sulu vary from -7.4 ‰ to 13.3 ‰ (ESM S1). In detail, average $\delta^{18}\text{O}(\text{Zrn})$ values for metaigneous rocks can be highly variable: 3.6 and 4.7 ‰ for metagabbros; from -7.4 to 10.0 ‰ for eclogites; from 3.0 to 6.7 ‰ for garnet amphibolites; and from -3.7 to 5.4 ‰ for orthogneisses, including one leucosome sample (#53). In contrast, there is a narrow range in $\delta^{18}\text{O}(\text{Zrn})$ for the granitic intrusions: from 3.5 to 4.5 ‰ for pegmatites and from 5.0 to 5.6 ‰ for granites and granodiorites. Zircons in paragneisses, quartzites, felsic granulites, and pelitic schists have average $\delta^{18}\text{O}$ values between 5.3 and 13.3 ‰. Overall, zircons have average $\delta^{18}\text{O}$ values, from -7.4 to 6.8 ‰ for the 17 samples from Sulu; from -3.6 to 7.5 ‰ for the Dabie samples (10); from -3.3 to 10.0 ‰ for the samples from Hong'an (18); and from -1.1 to 13.3 ‰ for the Tongbai samples (23). Average $\delta^{18}\text{O}(\text{Zrn})$ values for three samples (#70–72) from South Qinling vary from 6.8 to 8.5 ‰.

By comparison, many zircons in samples (#74–77) from the Baoxing Complex of southern Longmenshan in the South China Block are characterized by oscillatory zonation typical of igneous zircons as revealed by CL imaging. Some zircons in sample (#76) display core–rim structure, and the zircon rims are featureless. Spot analysis of twenty-three zircon grains in the four metagranite samples indicates a large variation in $\delta^{18}\text{O}$ of between 1.9 and 9.9 ‰ (Fig. 4). Average $\delta^{18}\text{O}$ values for the Baoxing samples range from 4.0 to 6.7 ‰ (ESM S1). One metarhyolite sample (#73) from the Yanjing Group in the same area has an average $\delta^{18}\text{O}(\text{Zrn})$ value as low as 3.9 ± 0.9 ‰. Zircon $\delta^{18}\text{O}$ for one sample (#78), from the Huangling granitoid in the South China Block, varies from 6.6 to 8.8 ‰, averaging 7.9 ± 1.8 ‰.

Zircons in two samples (#18 and #79) from the North China Block have an average $\delta^{18}\text{O}$ value of 5.7 ± 0.5 ‰ and 5.9 ± 0.4 ‰, respectively (ESM S1).

In situ U–Pb geochronology

Sixty-four out of 65 SIMS U–Th–Pb analyses of selected zircons from 19 samples from Dabie–Sulu indicate that there are two major $^{206}\text{Pb}/^{238}\text{U}$ age populations (Fig. 5a and ESM S4): (1) at 205 – 246 Ma ($n = 22$) for metamorphic zircon rims ($\text{Th}/\text{U} < 0.3$) and (2) 606 – 797 Ma ($n = 27$) for igneous zircon cores ($\text{Th}/\text{U} > 0.3$).

U–Th–Pb analysis of zircons from 49 samples by LA–ICP–MS was carried out in two separate sessions (ESM S5) to determine the (re-)crystallization age of the zircons, and data for five representative samples were

plotted on concordia diagrams (Fig. 5b–f). At Tongbai–Dabie–Sulu, zircons in eight out of 10 eclogite samples give Neoproterozoic ages for the igneous protoliths, and Triassic ages for the rims that resulted from syn-orogenic HP/UHP metamorphism. Zircons in one UHP eclogite sample (#19) from Dabie give discordia intercept ages of $1,924 \pm 17$ Ma and 231 ± 15 Ma (Fig. 5b), whereas metamorphic zircons in one HP eclogite sample (#30) from Hong'an give a weighted mean age of 305 ± 5 Ma ($n = 9$) (Fig. 5c). Likewise, zircons in 17 out of the 21 orthogneiss samples analyzed give Neoproterozoic protolith ages and Triassic rim ages that record syn-orogenic HP/UHP metamorphism (e.g., Fig. 5d). A few small igneous zircons (or cores) in four orthogneiss samples (#11, #25, #37, and #39) only give younger Paleozoic ages. Nevertheless, discordia upper intercept ages of 771 ± 86 and 752 ± 70 Ma on the concordia diagrams are obtained for both UHP eclogite and granitic orthogneiss samples from the same location (#37 and #39) (Wu et al. 2008a).

Zircons in one granite sample (#26) from Dabie give a weighted mean age of 752 ± 4 Ma ($n = 45$) (Fig. 5e), whereas zircons in a granodiorite sample (#69) from Tongbai give a weighted mean age of 454 ± 6 Ma ($n = 12$). The latter reflects the timing of arc magmatism in the region (e.g., Wang et al. 2011b).

Archean to Paleoproterozoic zircons have been preserved in paragneiss (#9), quartzite (#23), and felsic granulite (#27), whereas no zircons older than 600 Ma were determined in one paragneiss sample (#22). Zircons in a paragneiss sample (#28) from a Cretaceous dome at Dabie are as old as 3.0 Ga (ESM S1).

Zircons in samples from South Qinling and the South China Block (#70–78) give a weighted mean $^{206}\text{Pb}/^{238}\text{U}$ age or a discordant intercept age varying from 896 Ma to 775 Ma, reflecting the timing of magmatism (ESM S1; see Fig. 5f for #77). In contrast, zircons in two samples (#18 and #79) from the North China Block give a much older age, 2.91 Ga for magmatism and 1.84 Ga for metamorphism.

Discussion

Based on CL images and available U–Th–Pb data, we first attempt to distinguish Neoproterozoic “igneous” zircons from Triassic “metamorphic” zircons in the investigated rocks at Tongbai–Dabie–Sulu. We then investigate the origin of low- $\delta^{18}\text{O}$ Neoproterozoic igneous zircons or host igneous rocks in the region, using a comparison with Yellowstone caldera, USA, where similar oxygen signatures have been obtained. Finally, the geological implications of $\delta^{18}\text{O}$ for zircons of Archean to Cretaceous ages are discussed.

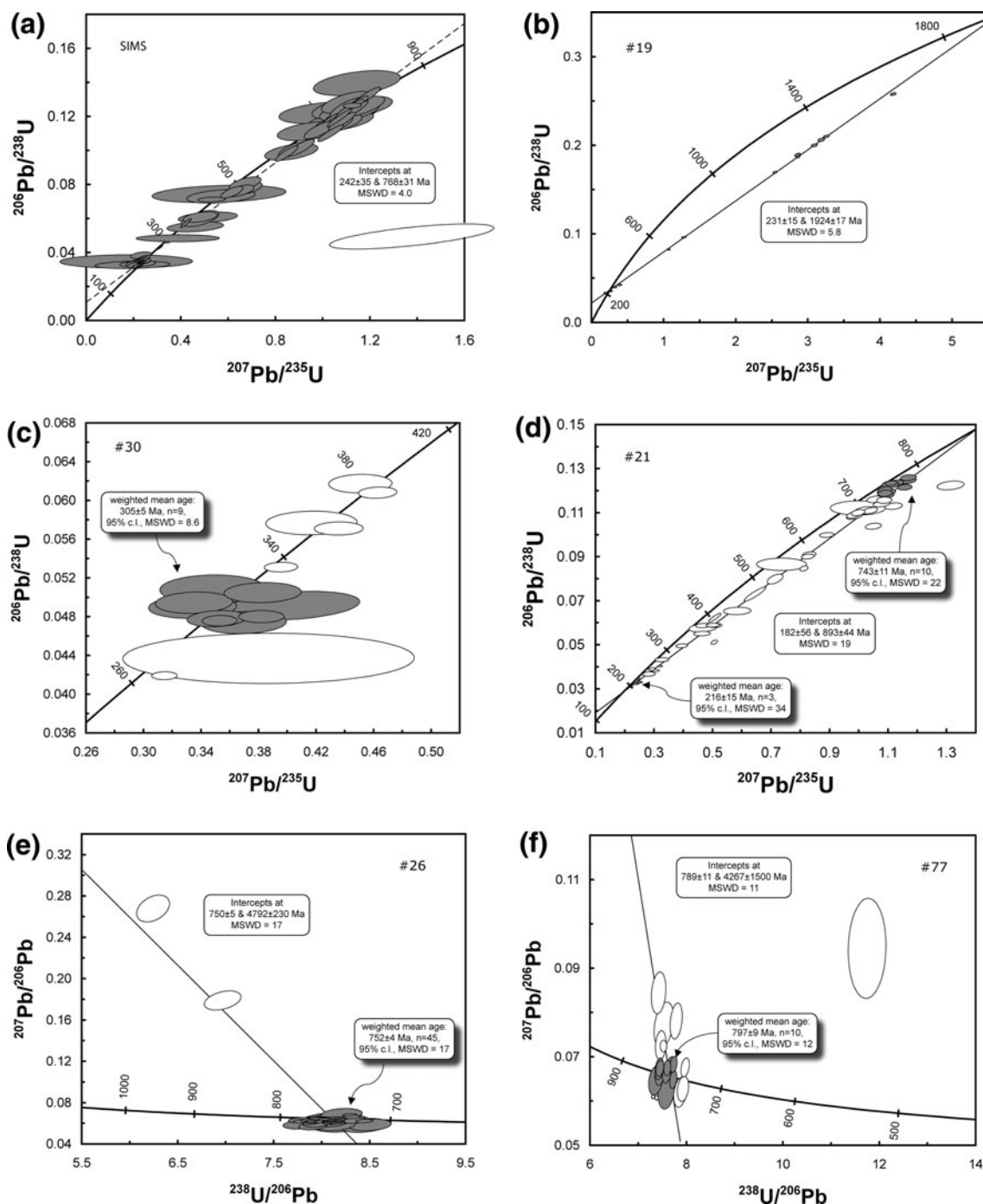


Fig. 5 Concordia diagrams for zircons in selected rock samples from the Qinling-Tongbai-Dabie-Sulu orogenic belt and adjacent areas, analyzed by: **a** ion microprobe (see Electronic supplementary materials or ESM S4), “false” discordia intercept ages for a total of

“Metamorphic” zircon versus “igneous” zircon

Both SIMS U–Th–Pb results (Liu et al. 2004, 2008, 2010a; Wallis et al. 2005; Cui et al. 2012; Hu et al. 2012; this study) and LA–ICP–MS U–Th–Pb results were plotted against SIMS $\delta^{18}\text{O}$ data for all zircon samples of this study

19 samples are given; and **(b–f)** laser ablation inductively coupled plasma mass spectrometry (ESM S5). Data-point error ellipses are 2 standard errors

from the Tongbai-Dabie-Sulu orogenic belt, including South Qinling, and from the South China and North China blocks (Fig. 6a). While both datasets are largely comparable, LA–ICP–MS age estimates are much younger or older than SIMS ages for a few zircons (ESM S6). In these cases, SIMS ages are preferred due to the very small

volume of material analyzed, comparable with SIMS $\delta^{18}\text{O}$ spots (cf. Chen et al. 2011; Sheng et al. 2012).

In general, Archean and Paleoproterozoic zircons have $\delta^{18}\text{O}$ values varying from 3.6 to 13.8 ‰, whereas younger zircons of Mesoproterozoic to Cretaceous age have a wide range in $\delta^{18}\text{O}$ between -10.8 and 12.0 ‰. It is noted that many Paleoproterozoic and Triassic zircons that have extremely low or high $\delta^{18}\text{O}$ values also have lower Th/U values than other zircons (see inset of Fig. 6a).

For many zircons from the Tongbai-Dabie-Sulu HP/UHP metamorphic rocks, the distinction between igneous cores and metamorphic rims may be verified because the cores commonly have higher Th/U ratios and give older U–Pb ages than the rims (e.g., Zheng et al. 2004; Chen et al. 2006). However, this may not always be the case, especially for those so-called metamorphosed protolith zircons variably recrystallized via the mechanisms of solid-state transformation or replacement alteration or dissolution–reprecipitation (e.g., Xia et al. 2009, 2010; Chen et al.

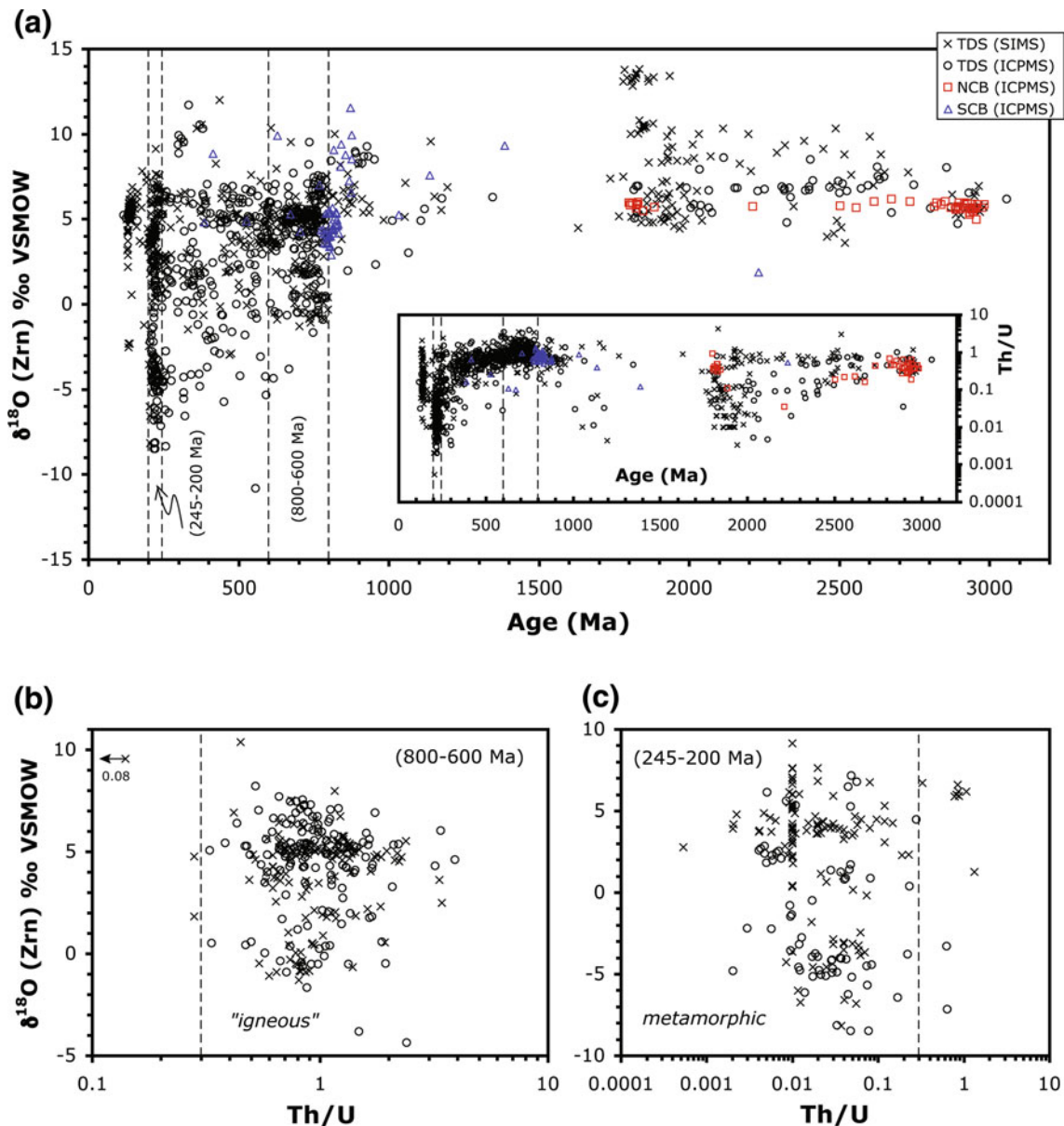


Fig. 6 Plots of in situ zircon $\delta^{18}\text{O}$ data versus U–Th–Pb results for all the investigated samples from the Qinling-Tongbai-Dabie-Sulu orogenic belt and adjacent areas. **a** $\delta^{18}\text{O}$ versus $^{206}\text{Pb}/^{238}\text{U}$ or $^{207}\text{Pb}/^{206}\text{Pb}$ age ($\geq 1,200$ Ma); **(b, c)** $\delta^{18}\text{O}$ versus Th/U for zircons with ages of 800–600 Ma and 245–200 Ma, respectively.

Abbreviations: *TDS* Qinling-Tongbai-Dabie-Sulu, *SCB* South China Block, *NCB* North China Block, *SIMS* ion microprobe, and *ICP-MS* (laser ablation) inductively coupled plasma mass spectrometry. Age data sources: Liu et al. (2004, 2008, 2010a), Wallis et al. (2005), Cui et al. (2012), Hu et al. (2012) and this study

2010, 2011; Sheng et al. 2012). In this study, only those zircons in HP/UHP metaigneous rocks from the Qinling-Tongbai-Dabie-Sulu orogenic belt that give ages between 800 and 600 Ma, equal to or close to the Neoproterozoic protolith age, are regarded as being “igneous” in origin, and most likely, they have preserved igneous protolith or parental magma oxygen isotope signatures. Given that three outliers (samples #2, #13, and #21) are excluded, “igneous” zircons of this age occur in both HP/UHP metaigneous rocks and Neoproterozoic granites that have Th/U ratios \geq ca. 0.3 and $\delta^{18}\text{O}$ values ≥ -1.7 ‰ (Fig. 6b). In contrast, most zircons with ages between 245 and 200 Ma, including those from syn-orogenic pegmatites (#10, #14, and #15; Wallis et al. 2005), have Th/U ratios \leq ca. 0.3 and highly variable $\delta^{18}\text{O}$ values ranging between -8.5 and 9.1 ‰ (Fig. 6c). In other words, there appears to be no difference in Th/U between Triassic pegmatite/granitic leucosome zircons and other contemporaneous HP/UHP metamorphic zircons (see also Liu et al. 2010b, 2012), in contrast to igneous zircons from other syn-orogenic intrusions, where the values are mostly ≥ 0.5 (e.g., Zhao et al. 2012). Metamorphic zircon is used here to describe those zircons (or zircon rims) newly formed from aqueous fluids or hydrous melts or where complete recrystallization of protolith zircons has occurred during Triassic metamorphism, including three different stages—prograde, peak-HP/UHP, and retrograde metamorphic stages—as demonstrated especially for UHP marbles and marble-hosted UHP eclogites at Dabie-Sulu (e.g., Liu et al. 2006a, b; Wu et al. 2006). Nine data points (Fig. 6c) for seven zircons with Th/U ratios $>$ ca. 0.3, from both eclogites (#32, #47, and #61) and orthogneisses (#3 and #25), are also omitted from further discussion. It should be pointed out that the contrasting Th/U ratios between Neoproterozoic “igneous” zircons and Triassic metamorphic zircons in this study are consistent with the results obtained using the same techniques (SIMS and LA-ICP-MS) for HP/UHP rocks, as well as Neoproterozoic granites in the region, that were compiled from the literature but not presented here.

Here we can assess $\delta^{18}\text{O}$ variability within a single grain in detail, for those zircons analyzed multiple times and for which age constraints are available. The intragrain $\delta^{18}\text{O}$ variability can be evaluated by using the following parameters: range in $\delta^{18}\text{O}$ within “igneous” or metamorphic zircon (or domain) and $\Delta^{18}\text{O}$ (M-Zrn-I-Zrn) for the variation in $\delta^{18}\text{O}$ between “igneous” zircons and metamorphic zircons from individual rock samples.

Metamorphic zircons in one retrograded eclogite sample (#66) have a narrow range in $\delta^{18}\text{O}$, between 3.2 and 4.2 ‰ ($n = 18$), with an identical average value (3.8 ‰) for two age-groups (223 versus 208 Ma; Liu et al. 2010a). This suggests that there is little or no oxygen isotopic shift in the

rock system from the peak metamorphic stage to the retrograde stage. Metamorphic zircons in two other samples (#33 and #39) are also relatively homogeneous in $^{18}\text{O}/^{16}\text{O}$, and they have an average $\delta^{18}\text{O}$ value of -3.3 ± 0.5 ‰ ($n = 10$) and 2.4 ± 0.7 ‰ ($n = 14$), respectively (ESM S1).

Available average $\delta^{18}\text{O}$ values for metamorphic zircons with ages between 245 and 200 Ma from other Tongbai-Dabie-Sulu rocks range from -8.3 to 6.8 ‰ (ESM S1). Only one pegmatite (#10) and four orthogneisses (#8, #11, #24, and #54) give a 2 SD value of ± 2.0 to ± 6.1 ‰ from the average calculation, indicating pronounced intergrain variability in $\delta^{18}\text{O}$.

The criteria for evaluation of oxygen isotopic equilibrium at *inter-* or *intracrystalline scale* vary according to the analytical method used in different studies. There are no available ion microprobe $\delta^{18}\text{O}$ (Grt) data for the Tongbai-Dabie-Sulu HP/UHP rocks, although certain intragrain $\delta^{18}\text{O}$ -variations in garnets from eclogites and granulite-facies metamorphic rocks elsewhere have been reported (Vielzeuf et al. 2005; Page et al. 2010; Russell et al. 2012). We can only utilize the laser fluorination results (ca. 300 μm spot size), which are indicative of gradients of $\delta^{18}\text{O}$ within garnets (ca. 1 cm in diameter) of no more than 1 ‰ (Xiao et al. 2001, 2002). Thus, we can use a $\delta^{18}\text{O}$ (M-Zrn) versus $\delta^{18}\text{O}$ (Grt) diagram to evaluate the oxygen isotopic equilibrium between metamorphic zircon and garnet only on a hand specimen scale by comparison between the average $\delta^{18}\text{O}$ values for metamorphic zircons ($n \geq 4$, 2 SD $\leq \pm 0.8$ ‰; SIMS) and the bulk data for garnets (laser fluorination). The equilibrium oxygen isotope fractionation between zircon and garnet is less than 0.2 ‰ at high temperatures (>600 °C; Zheng 1993a; Valley et al. 2003), and if these minerals equilibrated during peak-HP/UHP metamorphism, their oxygen isotope ratios should be nearly identical. All data points for five of the studied samples fall along the $\Delta = 0$ line in Fig. 3, and the $\Delta^{18}\text{O}$ (M-Zrn-Grt) values range between -0.2 and 0.2 ‰, within the analytical precision. These small $\Delta^{18}\text{O}$ (M-Zrn-Grt) values for a very limited number of samples suggest that approximate oxygen isotopic equilibrium between metamorphic zircon, like other eclogitic minerals, and garnet is attained and preserved during peak-HP/UHP metamorphism in these samples at the hand specimen scale and that the average $\delta^{18}\text{O}$ values for metamorphic zircons, $\delta^{18}\text{O}$ (M-Zrn), can be used to approximately estimate bulk composition of the host rock during metamorphism.

$\delta^{18}\text{O}$ for a few Neoproterozoic “igneous” zircon grains (or cores) varies by 2.6 – 7.7 ‰ (e.g., Fig. 2a, b). About one-third of Neoproterozoic “igneous” zircons, mostly from eclogites and orthogneisses, have a $\delta^{18}\text{O}$ value below 4 ‰ and down to -1.7 ‰ (Fig. 6b). The lowest $\delta^{18}\text{O}$ (<0) values are mainly from a Cretaceous leucosome (#53) in

dioritic orthogneiss enclosed in gneissic granite at Xinzhuang from the Tongbai Complex (Fig. 2d, c). This is the first ion microprobe report of such low- $\delta^{18}\text{O}$ igneous zircons (or cores) of Neoproterozoic age in rocks from Tongbai. Data for individual rock samples from other localities such as Qinglongshan–Hushan (Sulu; #1–4), Shuanghe (Dabie; #20 and #21), and Sidaohu (Hong'an; #37–39) are also shown in Fig. 7a, b for comparison. In a given sample, $\delta^{18}\text{O}$ for Neoproterozoic “igneous” zircon is commonly equal to or higher than that for Triassic metamorphic zircons or even Cretaceous igneous zircons.

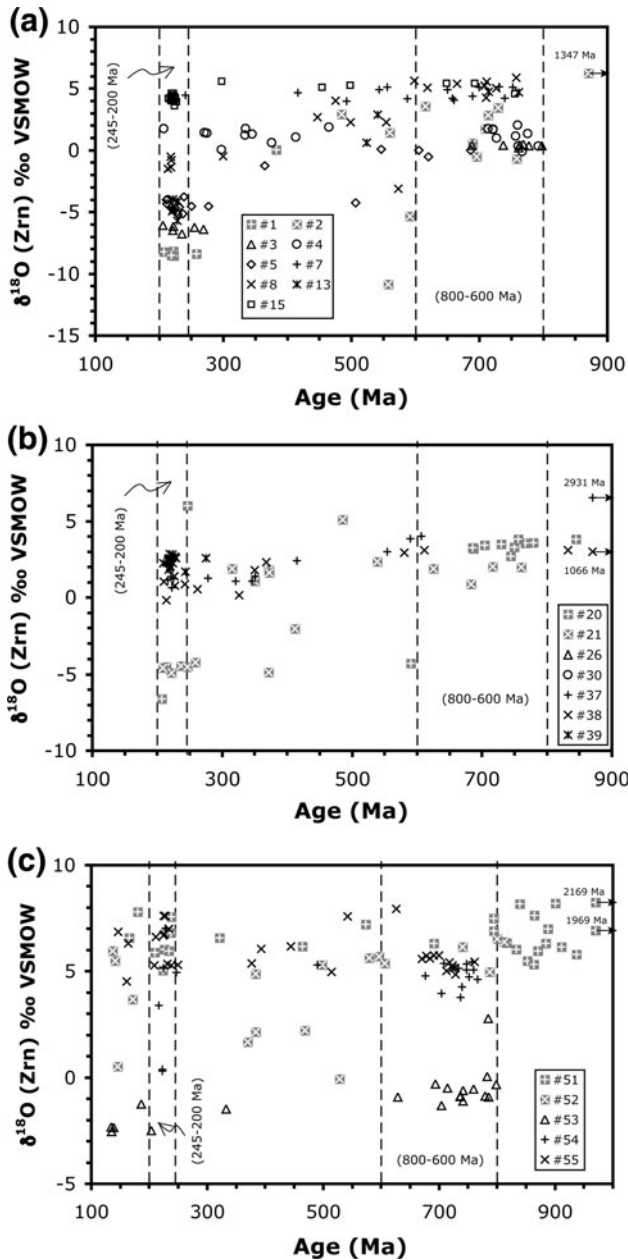


Fig. 7 Plots of in situ zircon $\delta^{18}\text{O}$ versus age for selected samples from the Tongbai-Dabie-Sulu orogenic belt: **a** Sulu; **b** Dabie and Hong'an (or W. Dabie); and **c** Tongbai

Average $\delta^{18}\text{O}$ values for Neoproterozoic “igneous” zircons (800–600 Ma) in samples from the Tongbai-Dabie-Sulu orogenic belt vary from -0.9 to 6.9 ‰; 2 SD is mostly $\leq \pm 2.1$ ‰ (ESM S1), some of which are lower than the value (5.3 ± 0.6 ‰) of zircon in equilibrium with a mantle-derived magma (Valley et al. 2005). Neoproterozoic “igneous” zircons in sample (#62) have a narrow range in $\delta^{18}\text{O}$, varying by only 0.6 ‰ (average = 4.7 ± 0.3 ‰, $n = 10$). Pronounced intergrain variability in $\delta^{18}\text{O}$ for Neoproterozoic “igneous” zircons is observed in two other samples (#2 and #26), as indicated by 2 SD up to ± 3.6 ‰ (ESM S1). To some extent, the more variable $\delta^{18}\text{O}$ values preserved in Neoproterozoic “igneous” than that of metamorphic zircons may be explained by either zircon inheritance or parental magma heterogeneity, if post-magmatic modifications that may be pronounced for zircons with ages between 600 and 245 Ma (Figs. 6a, 7) are precluded.

$\Delta^{18}\text{O}$ (metamorphic zircon–igneous zircon): Grouping the host rocks

A plot of $\delta^{18}\text{O}$ for “igneous” zircons versus $\delta^{18}\text{O}$ for metamorphic zircons can be used to show which rocks have been infiltrated by externally derived fluids. Figure 8a plots $\delta^{18}\text{O}$ for Triassic metamorphic zircon rims (245–200 Ma) versus Neoproterozoic “igneous” zircon cores (800–600 Ma), but only for some of the investigated samples due to limited data that allow correlation of age with $\delta^{18}\text{O}$ values. In addition, $\delta^{18}\text{O}$ values for zircons in a pegmatite (#15), metamorphic zircons without age constraints (2 SD $\leq \pm 1.2$ ‰, for average $\delta^{18}\text{O}$; ESM S1) from a UHP eclogite (#2) and two granitic orthogneisses (#4 and #20; Fig. 4) are also included in this diagram to enlarge the dataset. Here, a negligible deviation of average $\delta^{18}\text{O}$ of -6.4 ± 0.7 ‰ ($n = 17$) for metamorphic zircons in one of the samples (#20) from that for epidote (-6.5 ‰ in Fu et al. 1999) confirms approximate oxygen isotopic equilibrium between the two minerals at high temperatures (Zheng 1993a, 1993b).

Overall, Neoproterozoic “igneous” zircons from eclogites and orthogneisses commonly have equal or higher average $\delta^{18}\text{O}$ values than Triassic metamorphic zircons in the same samples. The data for metaigneous rocks can be split into four groups (I to IV) in Fig. 8a. Rocks of Group I have both Neoproterozoic “igneous” zircons and Triassic metamorphic zircons that have similar averaged $\delta^{18}\text{O}(\text{Zrn})$ values and approximate the mantle value of 5.3 ± 0.6 ‰ (Valley 2003). This group includes one orthogneiss sample (#55; and possibly #7, see Fig. 4) and one pegmatite sample (#15). Group II has similar $\delta^{18}\text{O}(\text{I-Zrn})$ to Group I, but significantly lower $\delta^{18}\text{O}(\text{M-Zrn or garnet})$: $\delta^{18}\text{O}(\text{M-Zrn}) = -4.5$ to 2.3 ‰,

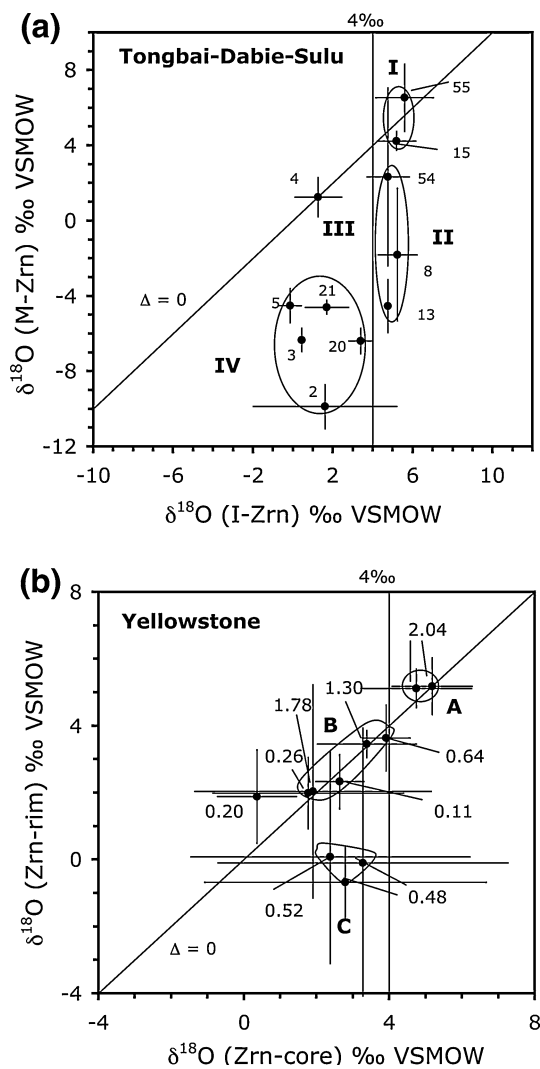


Fig. 8 δ - δ diagrams. **a** Plot of average $\delta^{18}\text{O}$ of Triassic metamorphic zircons (M-Zrn; 245–200 Ma) versus $\delta^{18}\text{O}$ of Neoproterozoic “igneous” zircons (I-Zrn; 800–600 Ma) from the same metaigneous rock samples at Tongbai-Dabie-Sulu. The number of individual analyses for average $\delta^{18}\text{O}$ calculation is ≥ 2 . Four groups (I–IV) of host metaigneous rocks have been identified: Group I, $\delta^{18}\text{O}(\text{M-Zrn}) \approx \delta^{18}\text{O}(\text{I-Zrn})$, 4.0–6.5 ‰; Group II, $\delta^{18}\text{O}(\text{M-Zrn})$, 0–4.0 ‰ and $\delta^{18}\text{O}(\text{I-Zrn})$, 4.0 to 6.5 ‰; Group III, $\delta^{18}\text{O}(\text{M-Zrn}) \approx \delta^{18}\text{O}(\text{I-Zrn})$, 0–4.0 ‰; Group IV, $\delta^{18}\text{O}(\text{M-Zrn}) \ll \delta^{18}\text{O}(\text{I-Zrn})$, –9.9 to 4.0 ‰. See Electronic supplementary materials S1 for sample details. **b** Plot of average $\delta^{18}\text{O}$ (± 2 SD) for igneous zircon rims (Zrn-rim) versus $\delta^{18}\text{O}$ for igneous zircon cores (Zrn-core), from individual rhyolitic samples from Yellowstone (Bindeman et al. 2008a). Three groups (A, B, and C) of host rhyolites have been identified. The numbers are ages (in Ma) of the rock samples. Uncertainties are plotted as ± 2 SD for multiple spot analyses and in many cases represent real sample-to-sample variability in $\delta^{18}\text{O}$

and $\delta^{18}\text{O}(\text{I-Zrn}) = 4.7$ to 5.2 ‰. Three orthogneiss samples (#8, #13, and #54) make up this grouping. Group III contains only one granitic orthogneiss sample (#4) that has low- $\delta^{18}\text{O}$ zircons that are equilibrated, $\delta^{18}\text{O}(\text{M-Zrn}) \approx \delta^{18}\text{O}(\text{I-Zrn}) < 4.0$ ‰. Rocks of Group IV are characterized

by much lower $\delta^{18}\text{O}$ values in Triassic metamorphic zircons than in Neoproterozoic “igneous” zircons (below 4 ‰), that is, $\Delta^{18}\text{O}(\text{M-Zrn-I-Zrn}) = -11.6$ to -4.3 ‰ and $\delta^{18}\text{O}(\text{M-Zrn}) = -9.9$ to -4.5 ‰. The rocks of Group IV are one UHP eclogite (#2) and four granitic orthogneisses (#3, #5, #20, and #21). Here, exceptionally high $\delta^{18}\text{O}$ values (6.3 to 9.5 ‰; Fig. 4) for one inherited zircon grain (no. 15) from the eclogite were omitted from the calculation.

As discussed above, $\delta^{18}\text{O}$ values of Triassic metamorphic zircon are approximately equilibrated with metamorphic garnet $\delta^{18}\text{O}$ values (Fig. 3), whereas $\delta^{18}\text{O}$ of Neoproterozoic “igneous” zircon cores record the $\delta^{18}\text{O}$ values of the original pre-metamorphic magmatic rocks. The $\delta^{18}\text{O}$ values of these latter zircons may also reflect the whole-rock $\delta^{18}\text{O}$ value at the time of crystallization, that is, during magmatism or earlier metamorphism (see Valley 2003; Page et al. 2007). Since the oxygen isotope index (I^{18}O) of a mineral relative to that of a reference mineral can be used to quantify the degree of ^{18}O -enrichment in the former, Zhao and Zheng (2002) were the first to demonstrate that the oxygen isotope index values increase with SiO_2 content from felsic to mafic to ultramafic rocks. For calc-alkaline plutonic rocks, the empirical oxygen isotopic fractionation between igneous zircon and the host magma, $\Delta^{18}\text{O}(\text{I-Zrn-WR})$, is approximately a linear function of SiO_2 composition (Lackey et al. 2008):

$$\Delta^{18}\text{O}(\text{I-Zrn-WR}) \approx -0.0612 \times (\text{wt.}\% \text{SiO}_2) + 2.5 \quad (1)$$

The effect of magmatic temperature on $\delta^{18}\text{O}(\text{I-Zrn})$ is relatively small (Valley 2003; Grimes et al. 2011).

Data points for two groups of metaigneous rock (Group I and Group III) fall near the $\Delta = 0$ line in Fig. 8a, suggesting approximate equilibration. Groups I and III therefore represent igneous rocks that intruded, crystallized, and were metamorphosed in a system that had no significant isotopic exchange with externally derived fluids or country rocks with contrasting $\delta^{18}\text{O}$ after the formation of igneous zircon, that is, at any stage between crystallization of the magma and HP/UHP metamorphism. In an igneous rock, other rock-forming minerals such as feldspar are less resistant than zircon to isotopic exchange during hydrothermal alteration (e.g., Cole and Chakraborty 2001; Valley 2003; Cole et al. 2004; Niedermeier et al. 2009), and the whole-rock $\delta^{18}\text{O}$ value decreases with hydrothermal alteration.

Data points for the two other groups of metaigneous rock (Groups II and IV) fall below the $\Delta = 0$ line in Fig. 8a, suggesting that minerals other than igneous zircons in the protoliths exchanged isotopes with surface waters at high temperature prior to crystallization of metamorphic

zircon. Among geologically important reservoirs, only surface waters are sufficiently low in $\delta^{18}\text{O}$ (ca. 0 for seawater and down to -40‰ for glacial meltwater; Hoefs 2004) to affect this exchange. The oxygen isotope fractionation between a mineral and water gets much smaller at higher temperatures, for example, $<\pm 1.5\text{‰}$ at $T > 700\text{ °C}$ for quartz or feldspar (O'Neil and Taylor 1967; Clayton et al. 1972; Zheng 1993a). The oxygen isotopic equilibrium between metamorphic zircon and garnet for many rocks argues against such fluid infiltration and/or significant diffusion under post-HP/UHP metamorphic conditions. Any post-UHP fluid–rock interactions would cause retrogression of the eclogitic rocks into amphibolite and/or greenschist-facies mineral assemblages and thus lead to retrograde oxygen isotope exchange during exhumation. Thus, rocks of Group II and Group IV were fluid-infiltrated after crystallization of the host magma and prior to HP/UHP metamorphism. This caused extensive hydrothermal alteration of the igneous protoliths by ancient meteoric water at high temperatures.

The low- $\delta^{18}\text{O}$ values for igneous zircon from rocks of Groups III and IV can be interpreted as resulting from remelting of hydrothermally altered wall rocks that exchanged with meteoric water at high temperatures prior to crystallization of later magma (e.g., Taylor 1986; Bindeman and Valley 2001). In other words, the mechanism to generate low- $\delta^{18}\text{O}$ magmas is through episodic intrusion and interaction with heated surface water where younger plutons melt previously altered, low- $\delta^{18}\text{O}$ wall rocks.

$\delta^{18}\text{O}(\text{Zrn})$ for other rocks, such as felsic granulite and metasedimentary rocks, is not shown in Fig. 8a due to poor age constraints. However, we recall results presented elsewhere in the literature where it was noted that higher $\delta^{18}\text{O}$ values for metamorphic than for igneous or detrital zircons [$\Delta^{18}\text{O}(\text{M-Zrn-I-Zrn})$, up to 7.1‰] are observed in Naxos, Greece (Martin et al. 2008), and the Adirondack Mountains, New York (Page et al. 2007; Lancaster et al. 2009). The significant increase in $\delta^{18}\text{O}$ from igneous core to metamorphic rim can be interpreted as resulting from metamorphic growth of zircon in oxygen isotopic equilibrium with contemporaneous high- $\delta^{18}\text{O}$ minerals in the host metasedimentary rocks via subsolidus reactions rather than by volume diffusion at high temperatures. This is in contrast to the results for zircons in metaigneous rocks at Tongbai-Dabie-Sulu, which commonly have negative $\Delta^{18}\text{O}(\text{M-Zrn-I-Zrn})$ values, suggesting post-magmatic, hydrothermal alteration of the igneous protoliths.

Genesis of Neoproterozoic low- $\delta^{18}\text{O}$ magmas: comparison with Yellowstone caldera

Worldwide, few low- $\delta^{18}\text{O}$ igneous zircons, that is, igneous zircons with $\delta^{18}\text{O}$ values below 4‰ , have been reported.

Where present, pristine low- $\delta^{18}\text{O}$ igneous rocks (or magmas) from young terranes that have $\delta^{18}\text{O}$ whole-rock values lower than primitive magma compositions or the mantle ($5.3 \pm 0.6\text{‰}$; Valley 2003) have been intensively studied, especially in shallow subvolcanic environments such as Heise, Yellowstone, Iceland, and the British Hebrides (e.g., Bindeman and Valley 2001; Monani and Valley 2001; Valley et al. 2005; Thirlwall et al. 2006; Bindeman et al. 2008a, b; Watts et al. 2011, 2012).

The presence of low- $\delta^{18}\text{O}$ igneous zircons in eclogite and granitic orthogneiss (Groups III and IV, Fig. 8a) requires a complex history to explain the pre-UHP ^{18}O -depletion. For comparison with Yellowstone caldera, we will use a two-stage ^{18}O -depletion model proposed by Fu et al. (2006) to illustrate the ^{18}O -depletion processes. In a similar model proposed by Wu et al. (2007) and Zheng et al. (2007a, 2008), two episodes of rift magmatism were invoked (at ca. 780 and ca. 760–750 Ma) throughout the Dabie and Sulu terranes rather than simply requiring repeated subcaldera magmatism at individual places to cause the extreme ^{18}O -depletion.

The processes proposed for Tongbai-Dabie-Sulu are essentially similar to those documented by analysis of $\delta^{18}\text{O}$ in zircons and quartz from rhyolites at Yellowstone caldera (Bindeman and Valley 2001; Bindeman et al. 2008a). The oxygen isotope fractionation between quartz and zircon yields the empirically or experimentally expected values for equilibrium at magmatic temperatures [$\Delta^{18}\text{O}(\text{Qz-Zrn}) = 2.5\text{--}1.8\text{‰}$ at $750\text{--}850\text{ °C}$; Valley et al. 2003; Trail et al. 2009] in high (normal) $\delta^{18}\text{O}(\text{Qz})$ ($4.1\text{--}7.9\text{‰}$) pre-caldera and extra-caldera lavas and tuffs at Yellowstone [average $\Delta^{18}\text{O}(\text{Qz-Zrn}) = 2.3 \pm 0.4\text{‰}$, $n = 21$; Bindeman and Valley 2001]. It is noted that the $\Delta^{18}\text{O}(\text{Qz-Zrn})$ values are lower than that estimated using the theoretical calibration of Zheng (1993a): $4.0\text{--}3.6\text{‰}$ at $750\text{--}850\text{ °C}$. In contrast, low- $\delta^{18}\text{O}$ lavas [$\delta^{18}\text{O}(\text{Qz}) \leq 2.7\text{‰}$] are characterized by low or reversed $\Delta^{18}\text{O}(\text{Qz-Zrn})$ values (down to -0.5‰ ; Bindeman and Valley 2001), which indicate isotopic disequilibrium. In other words, the low- $\delta^{18}\text{O}$ quartz phenocrysts have a lower $\delta^{18}\text{O}$ value than expected for equilibrium with zircon at high temperatures. This is interpreted to result from hydrothermal alteration of earlier crystallized magmas, which were remelted to form low- $\delta^{18}\text{O}$ lavas. However, zircons within these lavas include cores that were never altered and that preserve original higher $\delta^{18}\text{O}$ values and were cannibalized or recycled from the wall rocks (“cannibalism”: Bindeman and Valley 2001; Monani and Valley 2001).

Average $\delta^{18}\text{O}$ values for in situ analyses of igneous zircon cores are plotted versus igneous zircon rims in Fig. 8b (Table 2 of Bindeman et al. 2008a), for individual volcanic rock samples from Yellowstone. Three broad groups of rocks (A, B, and C) can be identified to illustrate

the subcaldera model. Group A includes two samples dated at 2.04 Ma that have mantle-like oxygen isotope ratios for igneous zircons (core and rim). Group B includes five samples that have an age between 1.78 and 0.11 Ma and where $\delta^{18}\text{O}(\text{I-Zrn rim}) \approx \delta^{18}\text{O}(\text{I-Zrn core}) \leq 4\text{‰}$. Group C includes three samples with an age of approximately 0.5 Ma, where $\delta^{18}\text{O}(\text{I-Zrn rim}) \ll \delta^{18}\text{O}(\text{I-Zrn core}) \leq 4\text{‰}$. Magmatism at Yellowstone started with the Group A, that is, 2.04 Ma. Low- $\delta^{18}\text{O}$ magmas formed at several stages. It is noted that an outlier (2.0 Ma) has an average $\delta^{18}\text{O}(\text{I-Zrn rim})$ higher than that of the igneous zircon cores.

The zircons in both the Tongbai-Dabie-Sulu metaigneous rocks (eclogite and granitic orthogneiss) and the Yellowstone rhyolites (Bindeman et al. 2008a) display core–rim structures as revealed by CL imaging, and the igneous zircon (or domain) $\delta^{18}\text{O}$ in both areas can be below 0, and even down to ca. -2‰ . However, one pronounced difference between the two areas is that zircon rims at Yellowstone are igneous, whereas zircon rims at Tongbai-Dabie-Sulu are metamorphic. Also, the volcanic rocks at Yellowstone have never been deeply buried, and based on Eq. 1, the average $\delta^{18}\text{O}$ zircon rim represents the oxygen isotope composition of magma after assimilation or melting of hydrothermally altered rocks. If such low- $\delta^{18}\text{O}$ igneous rocks were metamorphosed at high temperatures, newly formed metamorphic zircon could crystallize and would be in equilibrium with other low- $\delta^{18}\text{O}$ metamorphic minerals such as garnet or quartz (cf. Chen et al. 2011). Such low- $\delta^{18}\text{O}$ metaigneous rocks would thus be similar to the rocks of Groups II and IV at Tongbai-Dabie-Sulu (Fig. 8a).

Spatial distribution of Neoproterozoic low- $\delta^{18}\text{O}$ magmas in the South China Block

Neoproterozoic low- $\delta^{18}\text{O}$ (meta-) igneous rocks are widespread in the Tongbai-Dabie-Sulu orogenic belt. In addition to this study, a Neoproterozoic metagranite from Zaobuzhen (ZBZ in Fig. 1a) in the easternmost part of the Sulu terrane gives a $\delta^{18}\text{O}$ zircon value varying from -7.8‰ to -3.1‰ (bulk analysis) along a profile of 50 m length (Tang et al. 2008a). At Huangzhen in the South Dabie low-T/UHP eclogite-facies unit (HZ in Fig. 1b), low-T/high-P eclogites and associated granitic orthogneisses have $\delta^{18}\text{O}$ values as low as -4.3‰ for zircon and -6.3‰ for garnet (bulk analysis; e.g., Zheng et al. 1999; Li et al. 2004; Xia et al. 2008). A Neoproterozoic granite from Luzhenguan in North Dabie (LZG in Fig. 1b) that extends to the Beihuaiyang low-T/low-P greenschist-facies zone has a $\delta^{18}\text{O}(\text{Zrn})$ value of 0.6‰ (bulk analysis; Zheng et al. 2004), similar to that of the Danlongsi granite: -0.6 to 3.0‰ (bulk analysis; Wu et al. 2007) or $1.4 \pm 3.5\text{‰}$

(sample #26; ESM S1). Low- $\delta^{18}\text{O}$ UHP rocks at Sulu also occur down to depths of ca. 3 km from the surface, as determined from the CCSD-MH drill cores (e.g., Xiao et al. 2006; Chen et al. 2007). Although the presence of Neoproterozoic low- $\delta^{18}\text{O}$ igneous zircons in these rocks is yet to be confirmed by SIMS analysis, it appears that low- $\delta^{18}\text{O}$ magmas of Neoproterozoic age are not restricted to UHP units at Dabie-Sulu or the Tongbai Complex. If the Neoproterozoic low- $\delta^{18}\text{O}$ (meta-) igneous rocks are centers of pre-UHP metamorphic, paleo-hydrothermal systems, this may provide a key to reconstructing specific Neoproterozoic geological environments in the region.

The Neoproterozoic metaigneous rocks at Tongbai-Dabie-Sulu represent one of the largest terranes of low- $\delta^{18}\text{O}$ magmas known on Earth. If our model is correct, their wide distribution requires a protracted series of subcaldera events at a terrane scale because by volume the Tongbai-Dabie-Sulu orogenic belt is tens of times larger than the Yellowstone plateau (ca. $6,000\text{ km}^3$; Hildreth et al. 1991). The Snake River Plain, composed dominantly of felsic lavas, is the only known low- $\delta^{18}\text{O}$ magmatic terrane of comparable size. Given that the Dabie and Sulu terranes were joined prior to displacement of ca. 530 km along the sinistral Tancheng-Lujiang Fault (e.g., Okay and Sengör 1992), the distribution pattern of low- $\delta^{18}\text{O}$ rocks in the northern South China Block is considered to be linear. Thus, the linear trend and dimensions of low- $\delta^{18}\text{O}$ rocks at Tongbai-Dabie-Sulu are similar to the bimodal basaltic and silicic volcanism of the Neogene Snake River Plain—Yellowstone Plateau volcanic province, which is $>600\text{ km}$ long (e.g., Savov et al. 2009). The latter represents a single magmatic system (developed over 17 myr) that has been interpreted to result from an eastward-migrating Yellowstone hotspot relative to the North American plate (e.g., Leeman et al. 2008). It is noted that extensive crustal processes such as remelting of preexisting low- $\delta^{18}\text{O}$ crust, for example, meteoric-hydrothermal altered granitic rocks of the Idaho batholith, may also precede generation of the earliest rhyolite magmas especially in the central Snake River Plain (e.g., Borroughs et al. 2005, 2012; Leeman et al. 2008). The Isle of Skye within the British Tertiary Igneous Province is also regarded as recording a hotspot track (e.g., Stuart et al. 2000) and represents a comparably large low- $\delta^{18}\text{O}$ magmatic terrane (e.g., Monani and Valley 2001). We therefore propose that the Tongbai-Dabie-Sulu Neoproterozoic low- $\delta^{18}\text{O}$ igneous province may be related to a migrating hotspot relative to the South China Block during the Neoproterozoic. One may argue that there are no systematic age variations in the Neoproterozoic low- $\delta^{18}\text{O}$ igneous protoliths at Tongbai-Dabie-Sulu to support this hypothesis (ESM S1; see also Zheng et al. 2003, 2008, 2009). However, this would require further improved high-precision, high-accuracy geochronological research on

zircons, especially from pristine Neoproterozoic granitoids in order to resolve any small age differences, for example, by U–Pb chemical abrasion TIMS analysis (Mattinson 2005; Davydov et al. 2010). This would also help to better constrain the timing of Neoproterozoic magmatism in the region, and whether it was continuous or episodic.

Zircons with slightly low- $\delta^{18}\text{O}$ values are also present in both rhyolite of the Yanjing Group and granite of the Baoxing Complex (#73 and #77; Fig. 2e, f). This is also the first by SIMS reported at the western margin of the South China Block, where other Neoproterozoic igneous rocks, such as in the Pengguan, Xuelongbao, and Kangding complexes, are widespread (e.g., Zhou et al. 2002, 2006; Yan et al. 2008; Fig. 1d). Bulk analysis indicates that rocks from the Kangding Complex have mantle-like $\delta^{18}\text{O}(\text{Zrn})$ values of 4.2–6.2 ‰ (Zheng et al. 2007b) and that many samples from the Huangling Granitoid have $\delta^{18}\text{O}(\text{Zrn})$ values varying from 4.9 to 6.8 ‰ (Zhang et al. 2008, 2009). This is in contrast to the relatively high $\delta^{18}\text{O}(\text{Zrn})$ values (\geq ca. 7 ‰) for Neoproterozoic rocks from some other parts of the South China Block (Zheng et al. 2007b). Zhou et al. (2006) argue that, together with the arc signatures of other granites and mafic intrusions in the region, the 750-Ma Xuelongbao Adakitic Complex was likely derived from partial melting of a subducted oceanic slab. The Neoproterozoic mafic intrusions and granitoids of the Hannan and Micangshan massifs from the northwestern margin of the South China Block (i.e., South Qinling) are also interpreted to be subduction-related (e.g., Dong et al. 2011, 2012). In this regard, it appears that the western margin of the South China Block had a prolonged history of magmatism during the Neoproterozoic and that, like the present-day northern margin of the South China Block (i.e., the Tongbai-Dabie-Sulu orogenic belt), the slightly low- $\delta^{18}\text{O}$ zircons may also be attributed to extensive high-temperature hydrothermal alteration subsequent to either subduction-related or rift-related magmatism. However, so far no negative $\delta^{18}\text{O}$ zircons have been identified from rocks along the western margin of the South China Block, suggesting that the slightly low $\delta^{18}\text{O}$ values in this region more likely resulted from the involvement of high-temperature seawater in the hydrothermal alteration. This is the subject of ongoing investigations.

Wang et al. (2011a) reported that most low- $\delta^{18}\text{O}$ igneous zircons of detrital origin, extracted from four Cryogenian sedimentary rocks in the Nanhua Rift Basin, have ages of 800–700 Ma and that low- $\delta^{18}\text{O}$ igneous zircons started to appear from ca. 870 Ma, coinciding with the onset of extension and continental rifting. These authors argue that the occurrence of a sharp oxygen isotope shift from the highest $\delta^{18}\text{O}$ value of 12.2 ‰ (ca. 820 Ma) to the lowest of 2.0 ‰ (ca. 780 Ma) is contemporaneous with the onset of large-scale lithospheric extension and plume

activities in the South China Block. Zircons with the lowest- $\delta^{18}\text{O}$ (<4 ‰) values are further interpreted to have formed from remelting of 825–810 Ma igneous rocks related to the continental flood basalt event that isotopically exchanged with surface water at high temperatures (Wang et al. 2011c). When taken together, it is evident that many Neoproterozoic low- $\delta^{18}\text{O}$ igneous rocks in the South China Block indeed predate the well-documented Neoproterozoic glacial events (Zheng et al. 2007a, 2008; Wang et al. 2011a; this study). However, the potential involvement of recycled meltwaters from possible local continental glaciations, rather than the well-documented global Neoproterozoic glaciations, cannot completely be ruled out.

Geological implications

The $\delta^{18}\text{O}$ values for zircons formed during other magmatic and metamorphic events in the region and their geological significance are discussed here. The U–Pb ages of detrital zircons from quartzites (#23 and #63), paragneisses (#9, #28, #58, and #60), and pelitic schist (#50), as well as marble and felsic granulite from the Tongbai-Dabie-Sulu orogenic belt, support the conclusion that widespread Archean to Paleoproterozoic tectonothermal events took place at the northern margin of the South China Block (e.g., Ayers et al. 2002; Chen et al. 2003; Liu et al. 2006a, 2008, 2010a; Wu et al. 2006, 2008b; Sun et al. 2008; Jian et al. 2012; this study). In addition, many Paleoproterozoic metamorphic zircons (2.1–1.7 Ga) from paragneiss (#60) and pelitic schist (#50; see Fig. 2g, h) have relatively high $\delta^{18}\text{O}$ values of ca. 10 ‰ and ca. 13 ‰, respectively. In contrast, $\delta^{18}\text{O}$ for many other zircons of the same age, and the majority of Archean to early Paleoproterozoic zircons (>2.1 Ga) from other metasedimentary rocks, range from mantle-like values to higher than 6.5 ‰ (Fig. 6a). In combination with available hafnium isotope data (e.g., Wang et al. 2011c), this suggests episodic growth and reworking of older continental crust in the South China Block throughout geological time.

It appears that a consensus on the presence of recycled pre-collision oceanic crust in the Hong'an terrane has recently been reached (e.g., Wu et al. 2009; Liu et al. 2011 and references therein). In a HP eclogite (sample #30), metamorphic zircons with ages of 305 Ma have a $\delta^{18}\text{O}$ value of 9.5 ± 0.8 ‰ ($n = 5$), whereas $\delta^{18}\text{O}$ for two zircon grains (or domains) interpreted to be igneous, with ages of ca. 380 Ma, is as high as 10.5 ‰ (Fig. 2i, j). Other eclogite samples also from Xiong'dian have positive $\varepsilon_{\text{Nd}}(t)$ values (e.g., Jahn et al. 2005), distinct from the highly negative values of most of the Dabie-Sulu HP/UHP eclogites (e.g., Jahn et al. 1999 and references therein), and high $\delta^{18}\text{O}(\text{Grt})$ values (8.1–11.4 ‰; Fu et al. 2002; Jahn

et al. 2005). The $^{206}\text{Pb}/^{238}\text{U}$ zircon age for the Xiongdian HP eclogites varies from 424 to ca. 300 Ma (e.g., Jian et al. 2000; Gao et al. 2002; Sun et al. 2002; Cheng et al. 2009; Peters et al. 2012; this study). Moreover, zircons have initial epsilon Hf values [$\epsilon_{\text{Hf}}(t)$] of -11 to $+18$ (Peters et al. 2012). Thus, the Xiongdian eclogites could represent Middle Silurian–Early Devonian mafic volcanic rocks that record a different tectonic history from other HP/UHP metamorphic rocks in the Tongbai-Dabie-Sulu orogenic belt, although the presence of Proterozoic crustal components cannot be precluded. In this regard, the protolith likely formed part of ancient oceanic crust that may have experienced low-temperature seafloor alteration prior to Carboniferous HP metamorphism. While some of the altered basaltic rocks from mid-ocean ridges have whole-rock $\delta^{18}\text{O}$ value as high as 10 ‰ (Gregory and Taylor 1981; Eiler 2001), zircons appear to preserve the mantle-like $\delta^{18}\text{O}$ value (5.2–5.3 ‰; Cavosie et al. 2009; Grimes et al. 2011) and are resistant to seafloor hydrothermal alteration and/or low-T/HP metamorphism (Fu et al. 2012). In this scenario, newly crystallized metamorphic zircons from high- $\delta^{18}\text{O}$ altered rocks could have such high $\delta^{18}\text{O}$ values.

The average $\delta^{18}\text{O}(\text{Zrn})$ values of ca. 4.1 to 5.6 ‰ for post-orogenic intrusions or pegmatites at Tongbai (ESM S1) are consistent with the results of the previous studies: 3.9 to 7.7 ‰, for Cretaceous mafic–ultramafic rocks from Dabie (Xia et al. 2002; Zhao et al. 2005); and 3.2 to 6.4 ‰ for Cretaceous granites and diorites from Sulu (Huang et al. 2006). The incorporation of Neoproterozoic zircons, together with the lower $\delta^{18}\text{O}$ zircons in Cretaceous igneous rocks than primitive magma compositions, suggests that recycled Neoproterozoic hydrothermally altered supracrustal materials may be involved in post-orogenic magmatism in the area (e.g., Zhao et al. 2004, 2007; Huang et al. 2006; Xie et al. 2006; Dai et al. 2011).

Conclusions

Zircons in granite, pegmatite, metagabbro, eclogite, garnet amphibolite, granitic and dioritic orthogneiss, paragneiss, schist, quartzite, and felsic granulite from the Tongbai-Dabie-Sulu orogenic belt, east-central China, have been analyzed in situ for oxygen isotope ratio and age. Average $\delta^{18}\text{O}$ values for Triassic metamorphic zircons in the samples range from -9.9 to 6.8 ‰, whereas average $\delta^{18}\text{O}$ values for Neoproterozoic “igneous” zircon (800–600 Ma) vary from -0.9 to 6.9 ‰. Average $\Delta^{18}\text{O}$ values between metamorphic and “igneous” zircons vary from -11.6 to 0.9 ‰. The lowest $\delta^{18}\text{O}$ (down to ca. -2 ‰) Neoproterozoic “igneous” zircons (or cores) are mainly from Cretaceous leucosome in dioritic orthogneiss enclosed in

gneissic granite at Xinzhuang, Tongbai; this is the first ion microprobe report of such low- $\delta^{18}\text{O}$ Neoproterozoic igneous zircons (or cores) in the region.

A two-stage ^{18}O -depletion model is used to explain the formation of low- $\delta^{18}\text{O}$ magmas in the Tongbai-Dabie-Sulu orogenic belt, by analogy with the Yellowstone Plateau and the Isle of Skye, involving repeated subcaldera magmatic intrusion, exchange with heated meteoric water, and subsequent melting of altered wall rock. The widespread occurrence of Neoproterozoic low- $\delta^{18}\text{O}$ igneous protoliths at Tongbai-Dabie-Sulu and its comparable size (>600 km in length) to the Neogene Snake River Plain—Yellowstone Plateau volcanic province support the hypothesis that Neoproterozoic bimodal magmatism at Tongbai-Dabie-Sulu took place during continental rifting of the South China Block and may have been controlled by a migrating hotspot, similar to that at Yellowstone, relative to the continental crust.

Acknowledgments D.G. Chen, Z.H. Hou, S.B. Hu, B.P. Kohn, Y.T. Tian, S. Wallis, and Y.-F. Zheng provided many of the zircon separates or grain mounts. This work was supported initially by the U.S. National Science Foundation (EAR-0509639) and U.S. Department of Energy (93ER14389) and later by the University of Melbourne (ECR-600838). The WiscSIMS Laboratory is partly supported by NSF (EAR-0319230, EAR-0516725, EAR-0744079). BF gratefully acknowledges technical assistance of the AMMRF Flagship Ion Probe Facility (CMCA) at the University of Western Australia, funded by the University, State and Commonwealth Governments. Earlier versions of this manuscript have benefited greatly from thorough reviews by J.W. Valley, Y.-F. Zheng, and several anonymous referees.

References

- Ayers JC, Dunkle S, Gao S, Miller CF (2002) Constraints on timing of peak and retrograde metamorphism in the Dabie Shan ultrahigh-pressure metamorphic belt, east-central China, using U-Th-Pb dating of zircon and monazite. *Chem Geol* 186:315–331
- Baker J, Matthews A, Matthey D, Rowley D, Xue F (1997) Fluid-rock interactions during ultra-high pressure metamorphism, Dabie Shan, China. *Geochim Cosmochim Acta* 61:1685–1696
- BGMRSP (Bureau of Geology and Mineral Resources of Sichuan Province), (1991) Regional geology of Sichuan Province, People's Republic of China Ministry of Geology and Mineral Resources, Beijing. *Geol Mem Ser* 1(23):1–730 (in Chinese with English abstract)
- Bindeman I (2011) When do we need pan-global freeze to explain ^{18}O -depleted zircons and rocks? *Geology* 39:799–800
- Bindeman IN, Valley JW (2001) Low- $\delta^{18}\text{O}$ rhyolites from Yellowstone: magmatic evolution based on analyses of zircons and individual phenocrysts. *J Petrol* 42:1491–1517
- Bindeman IN, Fu B, Kita NT, Valley JW (2008a) Origin and evolution of silicic magmatism at Yellowstone based on ion microprobe analysis of isotopically zoned zircons. *J Petrol* 49:163–193
- Bindeman I, Gurenko A, Sigmarsson O, Chaussidon M (2008b) Oxygen isotope heterogeneity and disequilibria of olivine crystals in large volume Holocene basalts from Iceland: evidence

- for magmatic digestion and erosion of Pleistocene hyaloclastites. *Geochim Cosmochim Acta* 72:4397–4420
- Black LP, Kamo SL, Allen CM, Davis DW, Aleinikoff JN, Valley JW, Mundil R, Campbell IH, Korsch RJ, Williams IS, Foudoulis C (2004) Improved $^{206}\text{Pb}/^{238}\text{U}$ microprobe geochronology by monitoring of a trace-element-related matrix effect: SHRIMP, ID-TIMS, ELA-ICP-MS and oxygen isotope documentation for a series of zircon standards. *Chem Geol* 205:115–140
- Boroghs S, Wolff J, Bonnicksen B, Godchaux M, Larson P (2005) Large-volume, low- $\delta^{18}\text{O}$ rhyolites of the central Snake River Plain, Idaho, USA. *Geology* 33:821–824
- Boroughs S, Wolff JA, Ellis BS, Bonnicksen B, Larson P (2012) Evaluation of models for the origin of Miocene low- $\delta^{18}\text{O}$ rhyolites of the Yellowstone/Columbia River Large Igneous Province. *Earth Planet Sci Lett* 313–314:45–55
- Bowman JR, Moser DE, Valley JW, Wooden JL, Kita NT, Mazdab FK (2011) Zircon U-Pb isotope, $\delta^{18}\text{O}$ and trace element response to 80 m.y. of high temperature metamorphism in the lower crust: sluggish diffusion and new records of Archean craton formation. *Am J Sci* 311:719–772
- Burchfiel BC, Chen ZL, Liu YP, Royden LH (1995) Tectonics of the Longmen Shan and adjacent regions, central China. *Int Geol Rev* 37:661–735
- Cavosie AJ, Valley JW, Wilde SA, EIMF (2005) Magmatic $\delta^{18}\text{O}$ in 4400–3900 Ma detrital zircons: a record of the alteration and recycling of crust in the Early Archean. *Earth Planet Sci Lett* 235:663–681
- Cavosie AJ, Kita NT, Valley JW (2009) Magmatic zircons from the Mid-Atlantic Ridge: primitive oxygen isotope signature. *Am Mineral* 94:926–934
- Chen DG, Deloule E, Cheng H, Xia QK, Wu YB (2003) Preliminary study of microscale zircon oxygen isotopes for Dabie-Sulu metamorphic rocks: ion probe in situ analyses. *Chinese Sci Bull* 48:1670–1678
- Chen DG, Deloule E, Ni T (2006) Metamorphic zircon from Xindian eclogite, Dabie Terrain: U-Pb age and oxygen isotope composition. *Sci China (Ser D—Earth Sci)* 49: 68–76
- Chen RX, Zheng YF, Gong B, Zhao ZF, Gao TS, Chen B, Wu YB (2007) Oxygen isotope geochemistry of ultrahigh-pressure metamorphic rocks from 200–4000 m core samples of the Chinese Continental Scientific Drilling. *Chem Geol* 242:51–75
- Chen RX, Zheng YF, Xie LW (2010) Metamorphic growth and recrystallization of zircon: distinction by simultaneous in-situ analyses of trace elements, U-Th-Pb and Lu-Hf isotopes in zircons from eclogite-facies rocks in the Sulu orogen. *Lithos* 114:132–154
- Chen YX, Zheng YF, Chen RX, Zhang SB, Li QL, Dai MN, Chen L (2011) Metamorphic growth and recrystallization of zircons in extremely ^{18}O -depleted rocks during eclogite-facies metamorphism: evidence from U-Pb ages, trace elements, and O-Hf isotopes. *Geochim Cosmochim Acta* 75:4877–4898
- Cheng H, King RL, Nakamura E, Vervoort JD, Zheng YF, Ota T, Wu YB, Kobayashi K, Zhou ZY (2009) Transitional time of oceanic to continental subduction in the Dabie orogen: constraints from U-Pb, Lu-Hf, Sm-Nd and Ar-Ar multichronometric dating. *Lithos* 110:327–342
- CIGMR (Chengdu Institute of Geology and Mineral Resources), (2004) Geological map of Tibetan Plateau and Its Vicinity. Chengdu Map Press, Chengdu (in Chinese)
- Clayton RN, O'Neil JR, Mayeda TK (1972) Oxygen isotope exchange between quartz and water. *J Geophys Res* 77:3057–3067
- Cole DR, Chakraborty S (2001) Rates and mechanisms of isotopic exchange. In: Valley JW, Cole DR (eds) Stable isotope geochemistry. Mineralogical Society of America/Geochemical Society, Washington, DC. *Rev Mineral Geochem* 43:83–223
- Cole DR, Larson PB, Riciputi LR, Mora CI (2004) Oxygen isotope zoning profiles in hydrothermally altered feldspars: estimating the duration of water-rock interaction. *Geology* 32:29–32
- Cui JJ, Liu XC, Dong SW, Hu JM (2012) U-Pb and $^{40}\text{Ar}/^{39}\text{Ar}$ geochronology of the Tongbai complex, central China: implications for Cretaceous exhumation and lateral extrusion of the Tongbai–Dabie HP/UHP terrane. *J Asian Earth Sci* 47:155–170
- Dai LQ, Zhao ZF, Zheng YF, Li QL, Yang YH, Dai MN (2011) Zircon Hf-O isotope evidence for crust-mantle interaction during continental deep subduction. *Earth Planet Sci Lett* 308:229–244
- Davydov VI, Crowley JL, Schmitz MD, Poletaev VI (2010) High-precision U-Pb zircon age calibration of the global Carboniferous time scale and Milankovitch band cyclicity in the Donets Basin, eastern Ukraine. *Geochim Geophys Geosyst* 11: Q0AA04. doi:10.1029/2009GC002736
- Dong YP, Liu XM, Santosh M, Zhang XN, Chen Q, Yang C, Yang Z (2011) Neoproterozoic subduction tectonics of the northwestern Yangtze Block in South China: constraints from zircon U-Pb geochronology and geochemistry of mafic intrusions in the Hannan Massif. *Precambrian Res* 189:66–90
- Dong YP, Liu XM, Santosh M, Chen Q, Zhang XN, Li W, He DF, Zhang GW (2012) Neoproterozoic accretionary tectonics along the northwestern margin of the Yangtze Block, China: constraints from zircon U-Pb geochronology and geochemistry. *Precambrian Res* 196–197:247–274
- Eiler JM (2001) Oxygen isotope variations of basaltic lavas and upper mantle rocks. In: Valley JW, Cole DR (eds) Stable isotope geochemistry. Mineralogical Society of America/Geochemical Society, Washington, DC. *Rev Mineral Geochem* 43:319–364
- Fu B, Zheng YF, Wang ZR, Xiao YL, Gong B, Li SG (1999) Oxygen and hydrogen isotope geochemistry of gneisses associated with ultrahigh pressure eclogites at Shuanghe in the Dabie Mountains. *Contrib Mineral Petrol* 134:52–66
- Fu B, Zheng YF, Touret JLR (2002) Petrological, isotopic and fluid inclusion studies of eclogites from Sujiahe, NW Dabie Shan (China). *Chem Geol* 187:107–128
- Fu B, Kita NT, Valley JW (2006) Low- $\delta^{18}\text{O}$ magmas in the Dabie-Sulu UHP metamorphic terrains (China). *Geochim Cosmochim Acta* 70(18S): A186 (abstr)
- Fu B, Paul B, Cliff J, Bröcker M, Bulle F (2012) O-Hf isotope constraints on the origin of zircon in high-pressure mélange blocks and associated matrix rocks from Tinos and Syros, Greece. *Eur J Mineral* 24:277–287
- Gao S, Qiu YM, Ling WL, McNaughton NJ, Zhang BR, Zhang G, Zhang Z, Zhong Z, Suo ST (2002) SHRIMP single zircon U-Pb geochronology of eclogites from Yingshan and Xiongdian. *Earth Sci* 27:558–564 (in Chinese with English abstract)
- Gregory RT, Taylor HP Jr (1981) An oxygen isotope profile in a section of Cretaceous oceanic crust, Samail ophiolite, Oman: evidence for $\delta^{18}\text{O}$ buffering of the oceans by deep (>5 km) seawater-hydrothermal circulation at mid-ocean ridges. *J Geophys Res* 86:2737–2755
- Grimes CB, Ushikubo T, John BE, Valley JW (2011) Uniformly mantle-like $\delta^{18}\text{O}$ in zircons from oceanic plagiogranites and gabbros. *Contrib Mineral Petrol* 161:13–33
- Harrison TM, Schmitt AK, McCulloch MT, Lovera OM (2008) Early (≥ 4.5 Ga) formation of terrestrial crust: Lu-Hf, $\delta^{18}\text{O}$, and Ti thermometry results for Hadean zircons. *Earth Planet Sci Lett* 268:476–486
- Hellstrom J, Paton C, Woodhead J, Hergt J (2008) Iolite: software for spatially resolved LA-(QUAD and MC) ICPMS analysis. Mineralogical association of Canada Short Course series 40. Mineralogical Association of Canada, Vancouver, pp 343–348
- Hildreth W, Halliday AN, Christiansen RL (1991) Isotopic and chemical evidence concerning the genesis and contamination of

- basaltic and rhyolitic magma beneath the Yellowstone Plateau volcanic field. *J Petrol* 32:63–138
- Hoefs J (2004) *Stable isotope geochemistry*, 5th edn. Springer, Berlin
- Hu J, Liu XC, Qu W, Cui JJ (2012) Zircon U–Pb ages of Paleoproterozoic metabasites from the Tongbai Orogen and their geological significance. *Acta Geosci Sin* 33:305–315 (in Chinese with English abstract)
- Huang J, Zheng YF, Zhao ZF, Wu YB, Zhou HB, Liu XM (2006) Melting of subducted continent: element and isotopic evidence for a genetic relationship between Neoproterozoic and Mesozoic granitoids in the Sulu orogen. *Chem Geol* 229:227–256
- Ickert RB, Hiess J, Williams IS, Holden P, Ireland TR, Lanc P, Schram N, Foster JJ, Clement SW (2008) Determining high precision, in situ, oxygen isotope ratios with a SHRIMP II: analyses of MPI-DING silicate-glass reference materials and zircon from contrasting granites. *Chem Geol* 257:114–128
- Jahn BM, Wu FY, Lo CH, Tsai CH (1999) Crust–mantle interaction induced by deep subduction of the continental crust: geochemical and Sr–Nd isotopic evidence from post-collisional mafic-ultramafic intrusions of the northern Dabie complex, central China. *Chem Geol* 157:119–146
- Jahn BM, Liu X, Yui TF, Morin N, Bouhnik-Le Coz M (2005) High-pressure/ultrahigh-pressure eclogites from the Hong'an Block, East-Central China: geochemical characterization, isotope disequilibrium and geochronological controversy. *Contrib Mineral Petrol* 149:499–526
- Jeon H, Williams IS, Chappell BW (2012) Magma to mud to magma: rapid crustal recycling by Permian granite magmatism near the eastern Gondwana margin. *Earth Planet Sci Lett* 319–320:104–117
- Jian P, Liu DY, Yang WR, Williams IS (2000) Petrographic and SHRIMP studies of zircons from the Caledonian Xiong'dian eclogite, northwestern Dabie Mountains. *Acta Geol Sin* 74:766–773
- Jian P, Kröner A, Zhou GZ (2012) SHRIMP zircon U–Pb ages and REE partition for high-grade metamorphic rocks in the North Dabie complex: insight into crustal evolution with respect to Triassic UHP metamorphism in east-central China. *Chem Geol* 328:49–69
- Kelly J, Fu B, Kita NT, Valley JW (2007) Optically continuous silcrete quartz cements of the St. Peter Sandstone: high precision oxygen isotope analysis by ion microprobe. *Geochim Cosmochim Acta* 71:3812–3832
- Kemp AIS, Hawkesworth CJ, Foster GL, Paterson BA, Woodhead JD, Hergt JM, Gray CM, Whitehouse MJ (2007) Magmatic and crustal differentiation history of granitic rocks from Hf–O isotopes in zircon. *Science* 315:980–983
- Pidgeon RT, Furfaro D, Kennedy, AK, Nemchin AA, van Bronswijk W (1994) Calibration of zircon standards for the Curtin SHRIMP II. *United States Geol Surv Circ* 1107: 251 (abstr)
- Kita NT, Ushikubo T, Fu B, Valley JW (2009) High precision SIMS oxygen isotope analyses and the effect of sample topography. *Chem Geol* 264:43–57
- Lackey JS, Valley JW, Chen JH, Stockli DF (2008) Dynamic Magma systems, crustal recycling, and alteration in the Central Sierra Nevada Batholith: the oxygen isotope record. *J Petrol* 49:1397–1426
- Lancaster PJ, Fu B, Page FZ, Kita NT, Bickford ME, Hill BM, McLelland JM, Valley JW (2009) Genesis of metapelitic migmatites in the Adirondack Mts. New York. *J Metamorphic Geol* 27:41–54
- Leeman WP, Annen C, Dufek J (2008) Snake River Plain—Yellowstone silicic volcanism: implications for magma genesis and magma fluxes. In: Annen C, Zellmer GF (eds) *Dynamics of crustal magma transfer, storage and differentiation*. Geological Society, London. *Spec Publ* 304:235–259
- Li XP, Zheng YF, Wu YB, Chen FK, Gong B, Li YL (2004) Low-T eclogite in the Dabie terrane of China: petrological and isotopic constraints on fluid activity and radiometric dating. *Contrib Mineral Petrol* 148:443–470
- Liu FL, Liou JG (2011) Zircon as the best mineral for P–T–time history of UHP metamorphism: a review on mineral inclusions and U–Pb SHRIMP ages of zircons from the Dabie–Sulu UHP rocks. *J Asian Earth Sci* 40:1–39
- Liu FL, Xu ZQ, Liou JG, Katayama I, Masago H, Maruyama S, Yang JS (2002) Ultrahigh-pressure mineral inclusions in zircons from gneissic core samples of the Chinese Continental Scientific Drilling Site in eastern China. *Eur J Mineral* 14:499–512
- Liu XC, Jahn BM, Liu DY, Dong SW, Li SZ (2004) SHRIMP U–Pb zircon dating of a metagabbro and eclogites from western Dabieshan (Hong'an Block), China, and its tectonic implications. *Tectonophysics* 394:171–192
- Liu DY, Jian P, Kröner A, Xu ST (2006a) Dating of prograde metamorphic events deciphered from episodic zircon growth in rocks of the Dabie–Sulu UHP complex, China. *Earth Planet Sci Lett* 250:650–666
- Liu FL, Gerdes A, Liou JG, Xue HM, Liang FH (2006b) SHRIMP U–Pb zircon dating from Sulu–Dabie dolomitic marble, eastern China: constraints on prograde, ultrahigh-pressure and retrograde metamorphic ages. *J Metamorphic Geol* 24:569–589
- Liu YC, Li SG, Xu ST (2007) Zircon SHRIMP U–Pb dating for gneisses in northern Dabie high T/P metamorphic zone, central China: implications for decoupling within subducted continental crust. *Lithos* 96:170–185
- Liu XC, Jahn BM, Dong SW, Lou YX, Cui JJ (2008) High-pressure metamorphic rocks from Tongbaishan, central China: U–Pb and $^{40}\text{Ar}/^{39}\text{Ar}$ age constraints on the provenance of protoliths and timing of metamorphism. *Lithos* 105:301–318
- Liu XC, Jahn BM, Cui JJ, Li SZ, Wu YB, Li XH (2010a) Triassic retrograded eclogites and associated gneisses enclosed in Early Cretaceous gneissic granites from the Tongbai Complex, central China: constraints on the architecture of the HP/UHP Tongbai–Dabie–Sulu collision zone. *Lithos* 119:211–237
- Liu FL, Robinson PT, Gerdes A, Xue HM, Liu PH, Liou JG (2010b) Zircon U–Pb ages, REE concentrations and Hf isotope compositions of granitic leucosome and pegmatite from the north Sulu UHP terrane in China: constraints on the timing and nature of partial melting. *Lithos* 117:247–268
- Liu XC, Wu YB, Gao S, Wang J, Peng M, Gong HJ, Liu YS, Yuan HL (2011) Zircon U–Pb and Hf evidence for coupled subduction of oceanic and continental crust during the Carboniferous in the Huwan shear zone, western Dabie orogen, central China. *J Metamorphic Geol* 29:233–249
- Liu FL, Robinson PT, Liu PH (2012) Multiple partial melting events in the Sulu UHP terrane: zircon U–Pb dating of granitic leucosomes within amphibolite and gneiss. *J Metamorphic Geol* 30:887–906
- Ludwig KR (2001a) User's manual for Isoplot/Ex rev. 2.49: a geochronological toolkit for microsoft excel. Berkeley Geochronological Center special publication no. 1a
- Ludwig KR (2001b) SQUID 1.02, A user's manual. Berkeley Geochronological Center special publication no. 2
- Martin L, Duchêne S, Deloué E, Vanderhaeghe O (2008) Mobility of trace elements and oxygen in zircon during metamorphism: consequences for geochemical tracing. *Earth Planet Sci Lett* 267:161–174
- Mattinson JM (2005) Zircon U–Pb chemical abrasion (“CA-TIMS”) method: combined annealing and multi-step partial dissolution analysis for improved precision and accuracy of zircon ages. *Chem Geol* 220:47–66
- Monani S, Valley JW (2001) Oxygen isotope ratios of zircon: magma genesis of low $\delta^{18}\text{O}$ granites from the British Tertiary Igneous Province, western Scotland. *Earth Planet Sci Lett* 184:377–392

- Niedermeier DRD, Putnis A, Geisler T, Golla-Schindler U, Putnis CV (2009) The mechanism of cation and oxygen isotope exchange in alkali feldspars under hydrothermal conditions. *Contrib Mineral Petrol* 157:65–76
- Okay AI, Sengör AMC (1992) Evidence for intracontinental thrust-related exhumation of the ultra-high-pressure rocks in China. *Geology* 20:411–414
- O'Neil JR, Taylor HP Jr (1967) The oxygen isotope and cation exchange chemistry of feldspars. *Am Mineral* 52:1414–1437
- Page FZ, Ushikubo T, Kita NT, Riciputi LR, Valley JW (2007) High-precision oxygen isotope analysis of picogram samples reveals 2 μm gradients and slow diffusion in zircon. *Am Mineral* 92:1772–1775
- Page FZ, Kita NT, Valley JW (2010) Ion microprobe analysis of oxygen isotopes in garnets of complex chemistry. *Chem Geol* 270:9–19
- Paton C, Woodhead JD, Hellstrom JC, Hergt JM, Greig A, Maas R (2010) Improved laser ablation U-Pb zircon geochronology through robust downhole fractionation correction. *Geochem Geophys Geosyst* 11: Q0AA06. doi:10.1029/2009GC002618
- Peters TJ, Ayers JC, Gao S, Liu XM (2012) The origin and response of zircon in eclogite to metamorphism during the multi-stage evolution of the Huwan Shear Zone, China: insights from Lu-Hf and U-Pb isotopic and trace element geochemistry. *Gondwana Res.* doi:10.1016/j.gr.2012.05.008 (in press)
- Roger F, Malavieille J, Leloup PH, Calassou S, Xu Z (2004) Timing of granite emplacement and cooling in the Songpan-Garzê Fold Belt (eastern Tibetan Plateau) with tectonic implications. *J Asian Earth Sci* 22:465–481
- Rumble D, Yui TF (1998) The Qinglongshan oxygen and hydrogen isotope anomaly near Donghai in Jiangsu Province, China. *Geochim Cosmochim Acta* 62:3307–3321
- Rumble D, Giorgis D, Ireland T, Zhang ZM, Xu HF, Yui TF, Yang JS, Xu ZQ, Liou JG (2002) Low $\delta^{18}\text{O}$ zircons, U-Pb dating, and the age of the Qinglongshan oxygen and hydrogen isotope anomaly near Donghai in Jiangsu Province, China. *Geochim Cosmochim Acta* 66:2299–2306
- Russell AK, Kitajima K, Strickland A, Medaris LG Jr., Schulze DJ, Valley JW (2012) Eclogite-facies fluid infiltration: constraints from $\delta^{18}\text{O}$ zoning in garnet. *Contrib Mineral Petrol.* doi:10.1007/s00410-012-0794-9 (in press)
- Savov IP, Leeman WP, Lee CTA, Shirey SB (2009) Boron isotopic variations in NW USA rhyolites: Yellowstone, Snake River Plain, Eastern Oregon. *J Volcan Geotherm Res* 188:162–172
- Sheng YM, Zheng YF, Chen RX, Li QL, Dai MN (2012) Fluid action on zircon growth and recrystallization during quartz veining within UHP eclogite: insights from U-Pb ages, O-Hf isotopes and trace elements. *Lithos* 136–139:126–144
- Sláma J, Košler J, Condon DJ, Crowley JL, Gerdes A, Hanchar JM, Horstwood MSA, Morris GA, Nasdala L, Norberg N, Schaltegger U, Schoene B, Tubrett MN, Whitehouse MJ (2008) Plešovice zircon: a new natural reference material for U-Pb and Hf isotopic microanalysis. *Chem Geol* 249:1–35
- Stacey JS, Kramers JD (1975) Approximation of terrestrial lead isotope evolution by a two-stage model. *Earth Planet Sci Lett* 26:207–221
- Stuart FM, Ellam RM, Harrop PJ, Fitton JG, Bell BR (2000) Constraints on mantle plumes from the helium isotopic composition of basalts from the British Tertiary Igneous Province. *Earth Planet Sci Lett* 177:273–285
- Sun WD, Williams IS, Li SG (2002) Carboniferous and Triassic eclogites in the western Dabie Mountains, east-central China: evidence for protracted convergence of the North and South China Blocks. *J Metamorphic Geol* 20:873–886
- Sun M, Chen NS, Zhao GC, Wilde SA, Ye K, Guo JH, Chen Y, Yuan C (2008) U-Pb zircon and Sm-Nd isotopic study of the Huangtuling granulite, Dabie-Sulu belt, China: implication for the Paleoproterozoic tectonic history of the Yangtze craton. *Am J Sci* 308:469–483
- Tang J, Zheng YF, Wu YB, Gong B, Liu XM (2007) Geochronology and geochemistry of metamorphic rocks in the Jiaobei terrane: constraints on its tectonic affinity in the Sulu orogen. *Precambrian Res* 152:48–82
- Tang J, Zheng YF, Gong B, Wu YB, Gao TS, Yuan HL, Wu FY (2008a) Extreme oxygen isotope signature of meteoric water in magmatic zircon from metagranite in the Sulu Orogen, China: implications for Neoproterozoic rift magmatism. *Geochim Cosmochim Acta* 72:3139–3169
- Tang J, Zheng YF, Wu YB, Gong B, Zha XP, Liu XM (2008b) Zircon U-Pb age and geochemical constraints on the tectonic affinity of the Jiaodong terrane in the Sulu orogen, China. *Precambrian Res* 161:389–418
- Taylor HP Jr (1986) Igneous rocks: II. isotopic case studies of circumpacific magmatism. In: Valley JW, Taylor HP Jr, O'Neil JR (eds) *Stable isotopes in high temperature geological processes*. Mineralogical Society of America, Washington, DC. *Rev Mineral* 16:273–317
- Thirlwall MF, Gee MAM, Lowry D, Matthey DP, Murton BJ, Taylor RN (2006) Low $\delta^{18}\text{O}$ in the Icelandic mantle and its origins: evidence from Reykjanes Ridge and Icelandic lavas. *Geochim Cosmochim Acta* 70:993–1019
- Trail D, Mojzsis SJ, Harrison TM, Schmitt AK, Watson EB, Young ED (2007) Constraints on Hadean zircon protoliths from oxygen isotopes, Ti-thermometry, and rare earth elements. *Geochem Geophys Geosyst* 8:Q06014. doi:10.1029/2006GC001449
- Trail D, Bindeman IN, Watson EB, Schmitt AK (2009) Experimental calibration of oxygen isotope fractionation between quartz and zircon. *Geochim Cosmochim Acta* 73:7110–7126
- Valley JW (2001) Stable isotope thermometry at high temperatures. In: Valley JW, Cole DR (eds) *Stable isotope geochemistry*. Mineralogical Society of America/Geochemical Society, Washington, DC. *Rev Mineral Geochem* 43:365–413
- Valley JW (2003) Oxygen isotopes in zircon. In: Hanchar JM, Hoskin PWO (eds) *Zircon*. Mineralogical Society of America/Geochemical Society, Washington, DC. *Rev Mineral Geochem* 53:343–385
- Valley JW, Chiarenzelli JR, McLelland JM (1994) Oxygen isotope geochemistry of zircon. *Earth Planet Sci Lett* 126:187–206
- Valley JW, Kitchen N, Kohn MJ, Niendorf CR, Spicuzza MJ (1995) UWG-2, a garnet standard for oxygen isotope ratios: strategies for high precision and accuracy with laser heating. *Geochim Cosmochim Acta* 59:5223–5231
- Valley JW, Bindeman IN, Peck WH (2003) Empirical calibration of oxygen isotope fractionation in zircon. *Geochim Cosmochim Acta* 67:3257–3266
- Valley JW, Lackey JS, Cavosie AJ, Clechenko CC, Spicuzza MJ, Basei MAS, Bindeman IN, Ferreira VP, Sial AN, King EM, Peck WH, Sinha AK, Wei CS (2005) 4.4 billion years of crustal maturation: oxygen isotope ratios of magmatic zircon. *Contrib Mineral Petrol* 150:561–580
- Vielzeuf D, Champenois M, Valley JW, Brunet F, Devidal JL (2005) SIMS analysis of oxygen isotopes: matrix effects in Fe-Mg-Ca garnets. *Chem Geol* 223:208–226
- Wallis S, Tsuboi M, Suzuki K, Fanning M, Jiang LL, Tanaka T (2005) Role of partial melting in the evolution of the Sulu (eastern China) ultrahigh-pressure terrane. *Geology* 33:129–132
- Wang XC, Li ZX, Li XH, Li QL, Tang GQ, Zhang QR, Liu Y (2011a) Nonglacial origin for low- $\delta^{18}\text{O}$ Neoproterozoic magmas in the South China Block: evidence from new in-situ oxygen isotope analysis using SIMS. *Geology* 39:735–738
- Wang H, Wu YB, Gao S, Zhang HF, Liu XC, Gong HJ, Peng M, Wang J, Yuan HL (2011b) Silurian granulite-facies

- metamorphism, and coeval magmatism and crustal growth in the Tongbai orogen, central China. *Lithos* 125:249–271
- Wang XC, Li XH, Li ZX, Li QL, Tang GQ, Gap YY, Zhang QR, Liu Y (2011c) Episodic Precambrian crust growth: evidence from U-Pb ages and Hf-O isotopes of zircon in the Nanhua Basin, central South China. *Precambrian Res.* doi:10.1016/j.precamres.2011.06.001 (in press)
- Watson EB, Cherniak DJ (1997) Oxygen diffusion in zircon. *Earth Planet Sci Lett* 148:527–544
- Watts KE, Bindeman IN, Schmitt AK (2011) Large-volume rhyolite genesis in caldera complexes of the Snake River Plain: insights from the Kilgore Tuff of the Heise Volcanic Field, Idaho, with comparison to Yellowstone and Bruneau–Jarbridge rhyolites. *J Petrol* 52:857–890
- Watts KE, Bindeman IN, Schmitt AK (2012) Crystal scale anatomy of a dying supervolcano: an isotope and geochronology study of individual phenocrysts from voluminous rhyolites of the Yellowstone caldera. *Contrib Mineral Petrol* 164:45–67
- Wiedenbeck M, Alle P, Corfu F, Griffin WL, Meier M, Oberli F, Von Quadt A, Roddick JC, Spiegel W (1995) Three natural zircon standards for U-Th-Pb, Lu-Hf, trace element and REE analyses. *Geostand Newslett* 19:1–23
- Williams IS (1998) U-Th-Pb geochronology by ion microprobe. In: McKibben MA, Shanks III WC, Ridley WI (eds) Applications of microanalytical techniques to understanding mineralizing processes. Society of Economic Geologists, Littleton. *Rev Econom Geol* 7:1–35
- Woodhead J, Hergt J, Shelley M, Eggins S, Kemp R (2004) Zircon Hf-isotope analysis with an excimer laser, depth profiling, ablation of complex geometries, and concomitant age estimation. *Chem Geol* 209:121–135
- Woodhead J, Hellstrom J, Hergt J, Greig A, Maas R (2007) Isotopic and elemental imaging of geological materials by laser ablation Inductively Coupled Plasma mass spectrometry. *J Geostand Geoanal Res* 31:331–343
- Wu YB, Zheng YF, Zhao ZF, Gong B, Liu XM, Wu FY (2006) U-Pb, Hf and O isotope evidence for two episodes of fluid-assisted zircon growth in marble-hosted eclogites from the Dabie orogen. *Geochim Cosmochim Acta* 70:3743–3761
- Wu YB, Zheng YF, Tang J, Gong B, Zhao ZF, Liu XM (2007) Zircon U-Pb dating of water–rock interaction during Neoproterozoic rift magmatism in South China. *Chem Geol* 246:65–86
- Wu YB, Gao S, Zhang HF, Yang SH, Jiao WF, Liu YS, Yuan HL (2008a) Timing of UHP metamorphism in the Hong'an area, western Dabie Mountains, China: evidence from zircon U-Pb age, trace element and Hf isotope composition. *Contrib Mineral Petrol* 155:123–133
- Wu YB, Zheng YF, Gao S, Jiao WF, Liu YS (2008b) Zircon U-Pb age and trace element evidence for Paleoproterozoic granulite-facies metamorphism and Archean crustal rocks in the Dabie Orogen. *Lithos* 101:308–322
- Wu YB, Hanchar JM, Gao S, Sylvester PJ, Tubrett M, Qiu HN, Wijbrans JR, Brower FM, Yang SH, Yang QJ, Liu YS, Yuan HL (2009) Age and nature of eclogites in the Huwan shear zone, and the multi-stage evolution of the Qinling-Dabie-Sulu orogen, central China. *Earth Planet Sci Lett* 277:345–354
- Xia QK, Delouie E, Wu YB, Chen DG, Cheng H (2002) Oxygen isotopic compositions of zircons from pyroxenite of Daoshichong, Dabieshan: implications for crust-mantle interaction. *Chinese Sci Bull* 47:1466–1469
- Xia QX, Zheng YF, Zhou LG (2008) Dehydration and melting during continental collision; constraints from element and isotope geochemistry of low-T/UHP granitic gneiss in the Dabie Orogen. *Chem Geol* 247:36–65
- Xia QX, Zheng YF, Yuan HL, Wu FY (2009) Contrasting Lu-Hf and U-Th-Pb isotope systematics between metamorphic growth and recrystallization of zircon from eclogite-facies metagranite in the Dabie orogen, China. *Lithos* 112:477–496
- Xia QX, Zheng YF, Hu ZC (2010) Trace elements in zircon and coexisting minerals from low-T/UHP metagranite in the Dabie orogen: implications for action of supercritical fluid during continental subduction-zone metamorphism. *Lithos* 114:385–412
- Xiao YL, Hoefs J, van den Kerkhof AM, Li SG (2001) Geochemical constraints of the eclogite and granulite facies metamorphism as recognized in the Raobazhai complex from North Dabie Shan, China. *J Metamorphic Geol* 19:3–19
- Xiao YL, Hoefs J, van den Kerkhof AM, Simon K, Fiebig J, Zheng YF (2002) Fluid evolution during HP and UHP metamorphism in Dabie Shan, China: constraints from mineral chemistry, fluid inclusions and stable isotopes. *J Petrol* 43:1505–1527
- Xiao YL, Zhang ZM, Hoefs J, van den Kerkhof A (2006) Ultrahigh pressure metamorphic rocks from the Chinese Continental Scientific Drilling Project; II, Oxygen isotope and fluid inclusion distributions through vertical sections. *Contrib Mineral Petrol* 152:443–458
- Xie Z, Zheng YF, Zhao ZF, Wu YB, Wang ZR, Chen JF, Liu XM, Wu FY (2006) Mineral isotope evidence for the contemporaneous process of Mesozoic granite emplacement and gneiss metamorphism in the Dabie orogen. *Chem Geol* 231:214–235
- Yan DP, Zhou MF, Wei GQ, Gao JF, Liu SF, Xu P, Shi XY (2008) The Pengguan tectonic dome of Longmen Mountains, Sichuan Province: Mesozoic denudation of a Neoproterozoic magmatic arc-basin system. *Sci China (Series D, Earth Sci)* 51:1545–1559
- Ye K, Yao YP, Katayama I, Cong BL, Wang QC, Maruyama S (2000) Large areal extent of ultrahigh-pressure metamorphism in the Sulu ultrahigh-pressure terrane of East China: new implications from coesite and omphacite inclusions in zircon of granitic gneiss. *Lithos* 52:157–164
- Yui TF, Rumble D III, Lo CH (1995) Unusually low $\delta^{18}\text{O}$ ultra-high-pressure metamorphic rocks from the Su-Lu Terrain, eastern China. *Geochim Cosmochim Acta* 59:2859–2864
- Zhang SB, Zheng YF, Zhao ZF, Wu YB, Yuan HL, Wu FY (2008) Neoproterozoic anatexis of Archean lithosphere: geochemical evidence from felsic to mafic intrusives at Xiaofeng in the Yangtze George, South China. *Precambrian Res* 163:210–238
- Zhang SB, Zheng YF, Zhao ZF, Wu YB, Yuan HL, Wu FY (2009) Origin of TTG-like rocks from anatexis of ancient lower crust: geochemical evidence from Neoproterozoic granitoids in South China. *Lithos* 113:347–368
- Zhao ZF, Zheng YF (2002) Calculation of oxygen isotope fractionation in magmatic rocks. *Chem Geol* 193:59–80
- Zhao ZF, Zheng YF, Wei CS, Wu YB (2004) Zircon isotope evidence for recycling of subducted continental crust in post-collisional granitoids from the Dabie terrane in China. *Geophys Res Lett* 31: L22602 1–4
- Zhao ZF, Zheng YF, Wei CS, Wu YB, Chen FK, Jahn BM (2005) Zircon U-Pb age, element and C-O isotope geochemistry of post-collisional mafic-ultramafic rocks from the Dabie orogen in east-central China. *Lithos* 83:1–28
- Zhao ZF, Zheng YF, Wei CS, Wu YB (2007) Post-collisional granitoids from the Dabie orogen in China: zircon U-Pb age, element and O isotope evidence for recycling of subducted continental crust. *Lithos* 93:248–272
- Zhao ZF, Zheng YF, Zhang J, Dai LQ, Li QL, Liu XM (2012) Syn-exhumation magmatism during continental collision: evidence from alkaline intrusives of Triassic age in the Sulu orogen. *Chem Geol* 328:70–88
- Zheng YF (1993a) Calculation of oxygen isotope fractionation in anhydrous silicate minerals. *Geochim Cosmochim Acta* 57:1079–1091
- Zheng YF (1993b) Calculation of oxygen isotope fractionation in hydroxyl-bearing silicates. *Earth Planet Sci Lett* 120:247–263

- Zheng YF, Fu B, Gong B, Li S (1996) Extreme ^{18}O depletion in eclogite from the Su-Lu terrane in East China. *Eur J Mineral* 8:317–323
- Zheng YF, Fu B, Gong B, Xiao YL, Wei CS, Li SG (1998a) Oxygen isotope constraints on fluid flow during eclogitization in the Sulu terrane. *Prog Nat Sci* 8:98–105
- Zheng YF, Fu B, Li YL, Xiao YL, Li SG (1998b) Oxygen and hydrogen isotope geochemistry of ultrahigh pressure eclogites from the Dabie Mountains and the Sulu terrane. *Earth Planet Sci Lett* 155:113–129
- Zheng YF, Fu B, Xiao YL, Li YL, Gong B (1999) Hydrogen and oxygen isotope evidence for fluid-rock interactions in the stages of pre- and post-UHP metamorphism in the Dabie Mountains. *Lithos* 46:677–693
- Zheng YF, Fu B, Gong B, Li L (2003) Stable isotope geochemistry of ultrahigh pressure metamorphic rocks from the Dabie-Sulu orogen in China: implications for geodynamics and fluid regime. *Earth-Sci Rev* 62: 105–161
- Zheng YF, Wu YB, Chen FK, Gong B, Li L, Zhao ZF (2004) Zircon U-Pb and oxygen isotope evidence for a large-scale ^{18}O depletion event in igneous rocks during the Neoproterozoic. *Geochim Cosmochim Acta* 68:4145–4165
- Zheng YF, Wu YB, Gong B, Chen RX, Tang J, Zhao ZF (2007a) Tectonic driving of Neoproterozoic glaciations: evidence from extreme oxygen isotope signature of meteoric water in granite. *Earth Planet Sci Lett* 256:196–210
- Zheng YF, Zhang SB, Zhao ZF, Wu YB, Li XH, Li ZX, Wu FY (2007b) Contrasting zircon Hf and O isotopes in the two episodes of Neoproterozoic granitoids in South China: implications for growth and reworking of continental crust. *Lithos* 96:127–150
- Zheng YF, Gong B, Zhao ZF, Wu YB, Chen FK (2008) Zircon U-Pb age and O isotope evidence for Neoproterozoic low- $\delta^{18}\text{O}$ magmatism during supercontinental rifting in South China: implications for the snowball Earth event. *Am J Sci* 308:484–516
- Zheng YF, Chen RX, Zhao ZF (2009) Chemical geodynamics of continental subduction-zone metamorphism: insights from studies of the Chinese Continental Scientific Drilling (CCSD) core samples. *Tectonophysics* 475:327–358
- Zhou MF, Yan DP, Kennedy AK, Li YQ, Ding J (2002) SHRIMP U-Pb zircon geochronological and geochemical evidence for Neoproterozoic arc-magmatism along the western margin of the Yangtze Block, South China. *Earth Planet Sci Lett* 196:51–67
- Zhou MF, Yan DP, Wang CL, Qi L, Kennedy AK (2006) Subduction-related origin of the 750 Ma Xuelongbao adakitic complex (Sichuan Province, China): implications for the tectonic setting of the giant Neoproterozoic magmatic event in South China. *Earth Planet Sci Lett* 248:286–300
- Zhou JB, Wilde SA, Zhao GC, Zheng CQ, Jin W, Zhang XZ, Cheng H (2008) SHRIMP U-Pb zircon dating of the Neoproterozoic Penglai Group and Archean gneisses from the Jiaobei Terrane, North China, and their tectonic implications. *Precambrian Res* 160:323–340